Universidade de Aveiro Departamento de Química
2015

Vânia Filipa Martins Faustino

Extração e purificação de imunoglobulina G com sistemas aquosos bifásicos

Extraction and purification of immunoglobulin G with aqueous biphasic systems

Universidade de Aveiro Departamento de Química
2015

Vânia Filipa Martins Faustino

Extração e purificação de imunoglobulina G com sistemas aquosos bifásicos

Extraction and purification of immunoglobulin G with aqueous biphasic systems

Dissertação apresentada à Universidade de Aveiro para cumprimento dos requisitos necessários à obtenção do grau de Mestre em Biotecnologia, ramo de Biotecnologia Industrial e Ambiental, realizada sob a orientação científica da Doutora Mara Guadalupe Freire Martins, Investigadora Coordenadora do Departamento de Química, CICECO, da Universidade de Aveiro.

À mãe e ao pai …

o júri

Presidente

Prof. Dr. João Manuel da Costa Araújo Pereira Coutinho
Professor Catedrático do Departamento de Química, CICECO, da Universidade de Aveiro

Dr[a]. Mara Guadalupe Freire Martins
Investigadora Coordenadora do Departamento de Química, CICECO, da Universidade de Aveiro

Dr[a]. Ana Paula Mora Tavares
Estagiária de Pós-Doutoramento do Departamento de Química, CICECO, da Universidade de Aveiro

Agradecimentos

Um agradecimento especial à Dr[a]. Mara Freire pelo acompanhamento feito durante o desenvolvimento deste trabalho mas, principalmente, pela paciência e confiança depositadas em mim. À Ana Maria Conceição que me apoiou e acompanhou durante este tempo, e aturou por vezes os meus desânimos. Agradeço-lhe ainda pelas sugestões, pelo incentivo e dedicação. De superior a amiga passate, obrigada.

Um grande obrigado a todos os membros do Path e do Mini-Path, pelo apoio e por me terem acolhido tão bem. Agradeço especialmente à Maria João, Cláudia Leite, Rita Teles, Hugo Ferrão, Matheus Pereira e João Santos que tão bem me acolheram e me deram força nesta jornada.

A todos os colegas de Mestrado, um obrigado por serem pessoas tão bem dispostas, apesar do trabalho. À Teresa Dins que com a sua irona me fazia sempre sorrir.

Um grande obrigada ao Samuel Oliveira, Cátia Martins e Isabel que me acompanharam nesta caminhada tal como uma segunda família que mesmo nos momentos menos bons estiveram sempre presentes com o seu apoio e com um grande sorriso. Obrigada Soraia Mascarenhas e Beatriz Batista que fizeram parte de anos tão importantes da minha vida.

Joana Gomes, conheci-te nesta nova etapa das nossas vidas que chegou agora ao fim, mas agradeço por tal ter acontecido. Foste amiga, companheira, confidente. Obrigada por aturares os "stresses" que tão bem compreendias. Obrigada por seres quem és.

Obrigada Pai por sempre me apoiares e proporcionares que chegasse até aqui. Mãe obrigada por seres o espelho de uma mulher de força e coragem, e por me fazeres acreditar que eu seria capaz de terminar este longo caminho. Aos meus pais, sem eles, isto não seria possível. Aos irmãos que sempre estiveram do meu lado. Obrigada por acreditarem em mim, pelo vosso apoio e por estarem sempre dispostos a ajudar. Terminada esta jornada, hoje acredito que apesar de todas as dificuldades e desafios que a vida nos coloque, todos são capazes quando se tem um objectivo.

Palavras-chave

Anticorpos, imunoglobulina G, sistemas aquosos bifásicos, polímero, líquidos iónicos, extração, purificação.

Resumo

O sistema imunitário tem como ferramenta mais poderosa a produção de anticorpos, pois estes têm a capacidade de reconhecer e ligar-se a moléculas/organismos patogénicos. Atualmente, existem uma série de doenças que podem ser tratadas com anticorpos, nomeadamente com as imunoglobulinas G (IgG). Assim, o desenvolvimento de processos mais baratos e eficazes para a sua extração e purificação é uma área de interesse em biotecnologia. Os sistemas aquosos bifásicos (SAB) têm sido estudados para o efeito pois permitem a redução de custos e do número de passos envolvidos no processo, em comparação com os métodos convencionais. No entanto, os SAB tradicionais têm-se mostrado pouco seletivos, resultando em baixos fatores de purificação e rendimentos. Neste sentido, a incorporação de líquidos iónicos (LIs) nos SAB pode ser uma alternativa promissora para manipular a seletividade destes sistemas. Neste trabalho, estudaram-se SAB constituídos por polietileno glicol (PEG) de diferentes massas moleculares e um sal biodegradável (citrato de potássio), utilizando LIs como adjuvantes (5% m/m) para a extração de IgG de origem leporídea (coelho).

Inicialmente, estudaram-se o tempo de extração, o efeito da variação da massa molecular do PEG em solução tampão de $K_3C_6H_5O_7/C_6H_8O_7$ a pH≈7 e o efeito da variação de pH (5-9) sobre o rendimento (Y_{IgG}) e eficiência de extração (EE_{IgG}%) de IgG. Os melhores resultados obtidos em termos de EE_{IgG}% foram conseguidos com uma centrifugação a 1000 rpm durante 10 min para promover a separação de fases e equílibrio seguidos de 120 min de repouso. Este procedimento foi posteriormente aplicado aos restantes ensaios experimentais. Os resultados obtidos no estudo de PEGs de diferentes pesos moleculares revelaram uma elevada afinidade da IgG para a fase de PEG, principalmente com os PEGs de menor peso molecular (96% de EE_{IgG}% com o PEG 400). Por outro lado, a variação de pH da solução tampão não mostrou um efeito significativo sobre a EE_{IgG}%.

Por fim, foi avaliada a influência da adição de vários LIs (5% m/m) na extração de IgG nos SABs compostos por PEG 400 a pH≈7. Nestes estudos foi possível obter uma EE_{IgG}% de 100% com os LIs constituídos pelos aniões $[TOS]^-$, $[CH_3CO_2]^-$ e Cl^-, apesar dos Y_{IgG}% obtidos serem inferiores a 40%. Por outro lado, com LIs constituídos pelos aniões Br^-, assim como pelos catião $[C_{10}mim]^+$, não se conseguiram obter valores de 100% para a EE_{IgG}%, mas obtiveram-se melhores resultados em termos de Y_{IgG}%.

Os SAB constituídos por PEG, um sal orgânico biodegradável e LIs como adjuvantes revelaram-se um método alternativo e promissor para a purificação de IgG. No entanto, são necessários ainda estudos adicionais de modo a reduzir a perda de IgG durante o processo.

Keywords

Antibodies, immunoglobulin G, aqueous biphasic systems, polymer, ionic liquids, extraction, purification.

Abstract

The immune system is able to produce antibodies, which have the capacity to recognize and to bind to foreign molecules or pathogenic organisms. Currently, there are a diversity of diseases that can be treated with antibodies, like immunoglobulins G (IgG). Thereby, the development of cost-efficient processes for their extraction and purification is an area of main interest in biotechnology. Aqueous biphasic systems (ABS) have been investigated for this purpose, once they allow the reduction of costs and the number of steps involved in the process, when compared with conventional methods. Nevertheless, typical ABS have not showed to be selective, resulting in low purification factors and yields. In this context, the addition of ionic liquids (ILs) as adjuvants can be a viable and potential alternative to tailor the selectivity of these systems. In this work, ABS composed of polyethylene glycol (PEG) of different molecular weight, and a biodegradable salt (potassium citrate) using ILs as adjuvants (5 wt%), were studied for the extraction and purification of IgG from a rabbit source.

Initially, it was tested the extraction time, the effect on the molecular weight of PEG in a buffer solution of $K_3C_6H_5O_7/C_6H_8O_7$ at pH≈7, and the effect of pH (5-9) on the yield (Y_{IgG}) and extraction efficiency (EE_{IgG}%) of IgG. The best results regarding EE_{IgG}% were achieved with a centrifugation step at 1000 rpm, during 10 min, in order to promote the separation of phases followed by 120 min of equilibrium. This procedure was then applied to the remaining experiments. The results obtained in the study of PEGs with different molecular weights, revealed a high affinity of IgG for the PEG-rich phase, and particularly for PEGs of lower molecular weight (EE_{IgG}% of 96 % with PEG 400). On the other hand, the variation of pH in the buffer solution did not show a significant effect on the EE_{IgG}%.

Finally, it was evaluated the influence of the addition of different ILs (5% wt) on the IgG extraction in ABS composed of PEG 400 at pH≈7. In these studies, it was possible to obtain EE_{IgG}% of 100% with the ILs composed of the anions $[TOS]^-$, $[CH_3CO_2]^-$and Cl^-, although the obtained Y_{IgG}% were lower than 40%. On the other hand, the ILs composed of the anions Br^-, as well as of the cation $[C_{10}mim]^+$, although not leading to EE_{IgG}% of 100%, provide an increase in the Y_{IgG}%.

ABS composed of PEG, a biodegradable organic salt and ILs as adjuvants, revealed to be an alternative and promising method to purify IgG. However, additional studies are still required in order to reduce the loss of IgG.

Contents

List of tables

List of figures

List of symbols

% w/w or wt%: weight fraction percentage (%);

λ: wavelength (nm);

σ: standard deviation;

Abs: absorbance (dimensionless);

M_w: molecular weight ($g \cdot mol^{-1}$);

K_{OW}: octanol-water partition coefficient (dimensionless);

R^2: correlation coefficient (dimensionless);

α: ratio between the top weight and the total weight of the mixture (dimensionless);

$[PEG]$: concentration of PEG (wt % or $mol \cdot kg^{-1}$);

$[PEG]_{\mathrm{PEG}}$: concentration of PEG in the PEG-rich phase (wt %);

$[PEG]_{\mathrm{M}}$: concentration of PEG in the initial mixture (wt %);

$[Salt]$: concentration of salt (wt % or $mol \cdot kg^{-1}$);

$[Salt]_{\mathrm{IL}}$: concentration of salt in the ionic-liquid-rich phase (wt %);

$[Salt]_{\mathrm{Salt}}$: concentration of salt in the salt-rich phase (wt %);

$[Salt]_{\mathrm{M}}$: concentration of salt in the initial mixture (wt %);

$\mathrm{Abs}_{\mathrm{IL}}^{\mathrm{PEG}}$: absorbance of the IL solution, at the maximum wavelength, in the PEG-liquid-rich phase;

$\mathrm{Abs}_{\mathrm{IL}}^{\mathrm{Salt}}$*:* absorbance of the IL solution, at the maximum wavelength, in the salt-liquid-rich phase;

$EE_{IgG}\%$: percentage extraction efficiency of IgG (%);

Y_{IgG}: extraction yield of IgG;

K : partition coefficient (dimensionless);

K_{IgG}: partition coefficient of IgG (dimensionless);

K_{IL}: partition coefficient of IL (dimensionless).

List of abbreviations

ABS: aqueous biphasic system;

BP: bottom phase;

CDR: complementarity-determining region;

e.g.: *exempli gratia*;

Fab: fragment of antigen-binding;

Fc: fragment crystallizable region;

FDA: food and drug administration;

H: heavy chain;

HAS: human serum albumin;

HIC: hydrophobic interaction chromatography;

HIV: human immunodeficiency virus;

HPS: hydroxypropyl starch;

Ig: immunoglobulin;

IgG: immunoglobulin G;

IL: ionic liquid;

IVIG: intravenous IgG;

mAb: monoclonal antibobody;

Mw: molecular weight;

pAb: polyclonal antibody;

PEG: polyethylene glycol;

PPG: polypropylene glycol;

PVP: polyvinyl pyrrolidone;

SEC: size exclusion chromatography;

[C_2mim]Cl: 1-ethyl-3-methylimidazolium chloride;

[C_4mim]Cl: 1-butyl-3-methylimidazolium chloride;

[C_6mim]Cl: 1-hexyl-3-methylimidazolium chloride;

[C_8mim]Cl: 1-octyl-3-methylimidazolium chloride;

[C_{10}mim]Cl: 1-decyl-3-methylimidazolium chloride;

[C_{12}mim]Cl: 1-dodecyl-3-methylimidazolium chloride;

[C_{14}mim]Cl: 1-tetradecyl-3-methylimidazolium chloride;

[C_4mim]Br: 1-butyl-3-methylimidazolium bromide;

[C_4mim][TOS]: 1-butyl-3-methylimidazolium tosylate;

$[C_4mim][CH_3CO_2]$: 1-butyl-3-methylimidazolium acetate;

$[C_4mim][N(CN)_2]$: 1-butyl-3-methylimidazolium dicyanamide;

Ka: association constant;

L: light chains;

pI: isoelectric point;

TL: tie-line;

TLL: tie-line length;

TP: top phase;

V: variable region**;**

VR: volume ratio;

W_{PEG}: concentration of PEG

Y_{total}: total extraction yield;

Y_{TP}: extraction yield in the top phase**.**

1. General introduction

1.1. Scope and objectives

Humans are affected by many diseases, like cancer, immunodeficiency, chronic auto-immune diseases, infectious diseases, etc., for which an important alternative to their treatment could consist on the administration of monoclonal antibodies (mAbs) – passive immunotherapy. The US Food and Drug Administration (FDA) approved the first use of therapeutic mAbs in 1986, the Orthoclone OKT3 *(1)*, that was produced *in vivo* by hybridoma cells *(2)*. mAbs are used in high therapeutic doses, leading to an urgent increasing demand to obtain high quantities of pure mAbs. The production of therapeutic antibodies must met high standards of safety and efficiency, which translates into the requirement of high purity levels *(3)*. This purity challenge constitutes the major drawback in the global biopharmaceuticals market *(2)*.

The high cost of the currently used downstream technologies is the key problem preventing the widespread use of mAbs in passive immunotherapy, and therefore there is the need to develop effective, economical, and rapid methods for mAbs purification *(4)*. The typical approach used in the downstream processing of mAbs includes clarification, concentration, selective purification steps, and virus clearance (when produced by cells). Clarification, concentration and virus clearance contributes with about 10 % of the total downstream purification steps costs, which are between 20 and 60 %, and in some special cases, can go up to 90 % of the total production costs *(5,6)*. The purification is usually achieved by high-cost methodologies, such as chromatography, that are not viable in large-scale production.

In order to suppress these and other shortcomings related with the traditional methods, such as chromatography, the extraction and purification using aqueous biphasic systems (ABS) constitutes an interesting alternative. ABS are more viable than traditional methods due to the fact that clarification, concentration and partial purification of the target protein can be combined in a single unit operation *(2,7)*. The other great advantage is the fact that ABS are mostly composed of water and can be formed by combinations of polymers (such as polyethylene glycol, PEG) and organic salts (*e.g.*, potassium citrate), avoiding thus the use of organic, volatile and hazardous solvents *(8)*. However, these traditional polymer-salt systems present a restricted polarity range between the coexisting phases, which has been preventing high purity factors and yields to be achieved. To overcome this drawback, ionic liquids (ILs) can be used as phase-forming components of ABS. In fact, enhanced extractions, selectivities and recoveries have been achieved with IL-based ABS *(9)*. The use of ILs in ABS leads to the possibility of controlling the phases' polarities by an adequate choice of the constituting ions *(8)*, and so, this high tunability makes them a desirable class of extraction solvents in liquid–liquid extraction processes. In addition, it

was already shown that ILs can be used as adjuvants to tailor the selectivity and extraction aptitude for target biomolecules *(10)*. Therefore, the aim of this work consists on the use of polymer-salt-based ABS, with the use of ILs as adjuvants, for the extraction and purification of immunoglobulins G (IgG) from a rabbit source.

1.2. Antibodies

Antibodies or immunoglobulins, known as Ig's *(11)*, are glycoproteins present in the plasma and extracellular fluids (humors) which constitute the humoral branch of the animal immune system *(12–14)*. These active molecules are the first and the most important line of defense of the body immune system because they are produced by specialized B lymphocytes (white blood cells) in response to foreign and potentially toxic molecules or pathogens, known as antigens *(6)*.

B lymphocytes are responsible for the adaptive immunity, *i.e.*, they are originated and matured in the bone marrow, and each expresses a unique antigen-binding receptor on its membrane where each antibody has a binding specificity for particular antigens *(12)*. When these cells recognise and bind to an antigen, the cell divides itself rapidly, differentiating into memory B cells and effector B cells, called plasma cells *(14)*. Furthermore, this immunological response is heterogeneous resulting in many different cell lines of B lymphocytes producing antibodies to the same antigen *(15)*.

1.2.1. Antibody structure and function

Antibodies have a common structure with four polypeptides (Figure 1) found in many proteins, regardless of their specificity *(13,16)*. These four polypeptides, with an Y-shape, consist of two identical heavy chains (H) with a molecular weight of 50 kDa or more; and two identical light chains (L) with a molecular weight of 25 kDa each, resulting in a total molecular weight (immunoglobulin) of approximately 150 kDa *(13,15,16)*. Furthemore, each heavy and light chain are held together by a combination of non-covalent interactions to form a heterodimer (H-L) *(14,15)*. All four polypeptide chains contain variable (V) and constant (C) regions found at the amino and carboxyl terminal portions, respectively *(13)*.

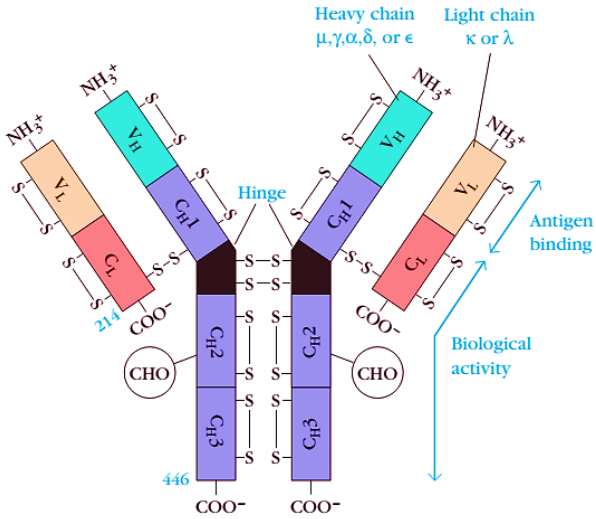

Figure 1: Schematic representation of the structure of an antibody: it contains an amino-terminal variable region (aqua and tan, respectively), and the constant regions (purple and red) (with limited variation that defines the two light-chain subtypes and the five heavy-chain subclasses). Some heavy chains (γ, δ, and α) also contain a proline-rich hinge region (black) *(14)*.

The constant region exhibits limited variation that defines the two light-chain subtypes and the five heavy-chain subclasses (α, μ, δ, ε, γ). Each of these five different heavy chains is called an isotype and these determine the class of antibody produced by the B cells (Figure 2): IgM(μ), IgG(γ), IgA(α), IgD(δ), or IgE(ε) (Table 1). These classes determine the type and the temporal nature of the immune response *(13,14,16)*, as well as the effector functions *(11)*.

Table 1: Chain composition of the five immunoglobulin classes in humans *(14)*.

Class	Heavy chain	Subclasses	Light chain	Formula
IgG	γ	γ1, γ2, γ3, γ4	κ or λ	$\gamma_2\kappa_2$
				$\gamma_2\lambda_2$
IgM	μ	None	κ or λ	$(\mu_2\kappa_2)_n$
				$(\mu_2\lambda_2)_n$
				n = 1 or 5
IgA	α	α1, α2	κ or λ	$(\alpha_2\kappa_2)_n$
				$(\alpha_2\lambda_2)_n$
				n = 1, 2, 3 or 4
IgE	ϵ	None	κ or λ	$\epsilon_2\kappa_2$
				$\epsilon_2\lambda_2$
IgD	δ	None	κ or λ	$\delta_2\kappa_2$
				$\delta_2\lambda_2$

The hypervariable regions, called *complementarity-determining regions* (CDRs), are dependent and determine the antibody specificity *(11)*. These regions are located between the amino-terminal of light and heavy regions, with a molecular weight of 50 kDa, and these segments are the first 110 amino-acids of the chain. Moreover, these regions correspond to the region where the amino-terminal groups join to form two identical antigen binding-sites (Figure 3) (binding to the epitope), called Fab ("fragment of antigen-binding") *(14,16)*. Each Fab fragment can bind to an antigen, and as two Fab fragments are present in the antibody, each antibody molecule is at least bivalent *(16)*. Furthemore, there are also the carboxy terminal regions of the two heavy chains (tail) fold together in order to create the Fc domains or crystallizable fractions, and these have a molecular weight of 50 kDa and no antigen binding activity. The Fc is also responsible for the Ig biological functions, like natural killer cell activation, classical complement pathway activation and phagocytosis *(14,16)*. These two arms (Fab) and the tail (Fc) are linked by a region rich in proline, threonine and serine, called the hinge, that provides the ability of the antibody to interact with a variety of antigens, due to its lateral and rotational movement *(16)*.

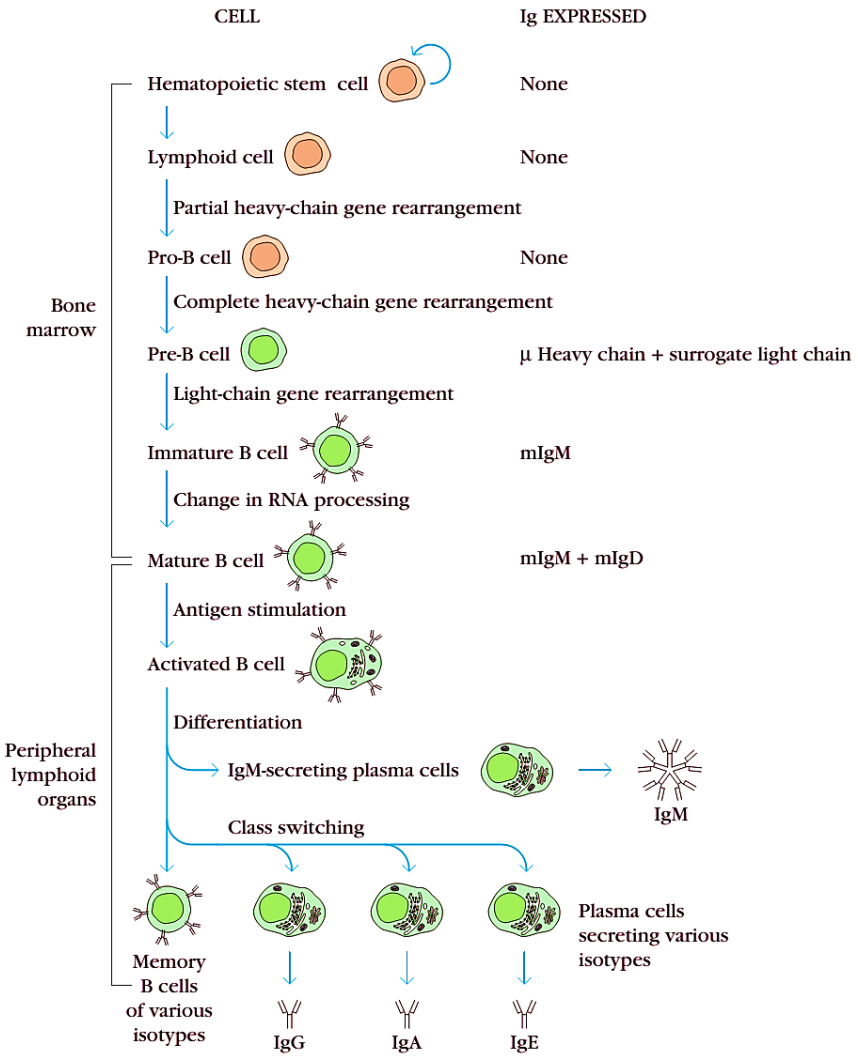

Figure 2: Development of B-cells, in which mature B cells are activated and differentiated in presence of an antigen. mIgM and mIgD are membrane-associated Ig's; IgG, IgA, and IgE are secreted immunoglobulins *(14)*.

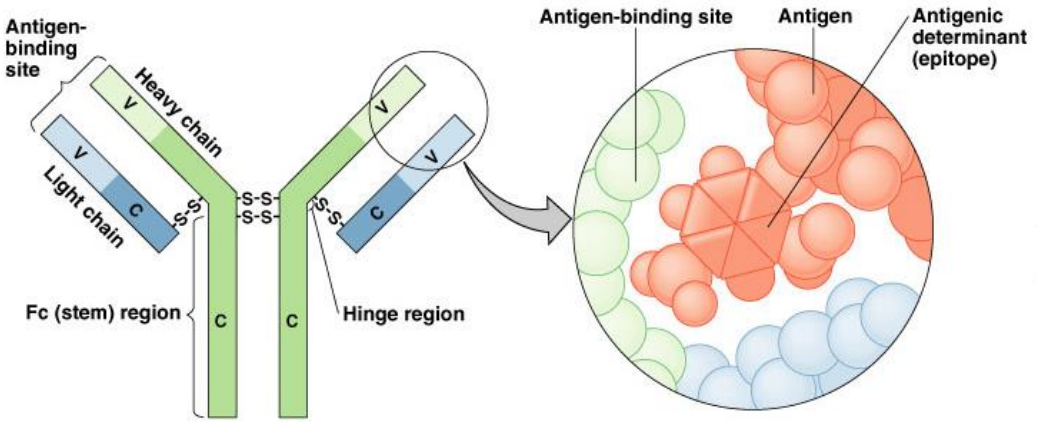

Figure 3: Amino-terminal portions corresponding to the variable regions of the antibody that bind to an antigen *(16)***.**

The antibodies importance is mostly related with their function and/or binding specificity for specific antigens *(16)*. Neverthless, antibodies have three functions: the binding versatility, the binding specificity, and the biological activity *(11)*. In response to a particular antigen, antibodies produced by a single B cell clone is termed a monoclonal antibody; if they are produced by a mixture of various B lymphocyte clones they are termed polyclonal antibodies *(12)*. In this work, polyclonal antibodies from rabbit serum were investigated.

1.2.2. Polyclonal and monoclonal antibodies

The monoclonal antibodies (mAbs) are antibodies of a single idiotype secreted by one clone of B lymphocytes, *i.e.*, a single hybridoma reacts with the same epitope on antigens *(11,12,16)*. The somatic cells hybridization was described for the first time by Georges J. F. Köhler and César Milstein in 1975 *(17)*. On the other hand, polyclonal antibodies (pAbs) are heterogeneous, since they represent a collection of antibodies secreted by different B cell lineages, allowing them to recognize multiple epitopes of the same antigen *(16)*. pAbs are acquired from serum and comprise heterogeneous and more complex mixtures of antibodies of different affinities. On the other hand, mAbs are produced *in vitro,* using for instance Chinese hamster ovary (CHO) cells *(18)*.

The pAbs and mAbs have their advantages and disadvantages in terms of generation, cost, and overall applications *(19)*. Both play an important role, with several applications in biology, biomedical research, diagnosis and therapy *(3,12)*. mAbs have some disadvantages in relation to pAbs, such as a higher susceptibility to small changes in pH and salt concentration *(16)*. Furthermore, the production of mAbs is time-consuming, since from the immunization until the

establishment of a cloned cell line it can take from 3 to 6 months *(19)*. The production of pAbs can be less time-consuming and less expensive. However, the immunization and response of the mammal cannot be discarded.

The mAbs also have effector functions, and thus they cannot produce the desired biologic response, such as a readily activation of the complement, and precipitation or agglutination of antigens *(11)*. mAbs also display monospecificity that limits their usefulness since small changes in the structure of an epitope can markedly affect their function. Therefore, mAbs are less tolerant to minor changes in the antigen (polymorphism, heterogeneity of glycosylation, or slight denaturation) *(16)*. However, the attractive specificity of mAbs is an extremely important feature in a great array of clinical laboratory diagnostic tests, such as in detecting and identifying serum analytes, cell markers, and pathogenic agents, among others *(19)*. Moreover, mAbs have also other advantages as their homogeneity, which it is useful in evaluating changes in molecular conformation and protein-protein interactions *(16)*. Moreover, a continuous culture of a single clone of B cell hybridomas offers a reproducible supply of antibodies *(19)*. On the other hand, pAbs offer additional vantages compared with mAbs, such as the capability to recognize multiple epitopes and their tolerance to minor changes in the antigen (*e.g.,* polymorphism, heterogeneity of glycosylation or slight denaturation).

Nowadays, mAbs are used in the treatment of several diseases and have an enormous utility in diagnosis and immunologic investigations *(14,19,20)*. The mAbs market is under a fastest growing and is amongst the most lucrative in the biopharmaceuticals industry *(21)*. More than 26 monoclonal antibody-based therapeutics were already approved by the FDA *(6,20,21)*, and according to a recent report from The Antibody Society (2013/2/28), 36 other therapeutic mAbs are in clinical trials *(13)*. Thus, mAbs constitute the largest product segment in the biopharmaceuticals market with an estimated share of 25.6% in 2013, and accounting with US$51.1 billion *(2,21)*.

Within the wide range of therapeutic mAbs and pAbs, one particular type of antibodies, namely IgG, are amongst the most potent effector molecules of the humoral immunity and play an essential role in the recognition of foreign proteins. Hence, they are increasingly being used as alternative drugs to treat many diseases *(22)*.

1.3. IgG structure and molecular characteristics

IgG is the main class of antibodies present in the blood, lymph, peritoneal, and cerebro-spinal fluids *(23)*, and constitute about 20 % of the total plasma proteins, with a total concentration in

blood within 10–25 mg/mL *(22,24)*. The basic unit of all IgGs (Figure 4) consists of four polypeptide chains, comprising two identical light chains (either κ or λ) and two identical heavy chains (γ) *(11,24)*. These chains are held together by non-covalent and covalent bindings (interchain disulfide bridges), and their sctruture resembles the letter Y with a well-defined globular structure *(24)*.

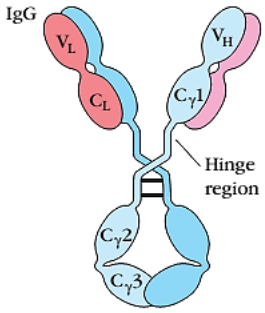

Figure 4: IgG structure: light chains (shades of red), disulfide bonds (thick black lines), heavy chains (blue and purple) *(14)*.

In 1960, four subclasses of IgG in human blood were identified: IgG1, IgG2, IgG3 and IgG4 (in a decreasing order of abundance) (Figure 5) *(25)*. Although all subclasses share a common genetic basis and have the same size and conformation, they differ in the specific sequence of amino acids in the variable domains (*i.e.*, the antigen-binding domains, Fab) *(11,22,24)*.

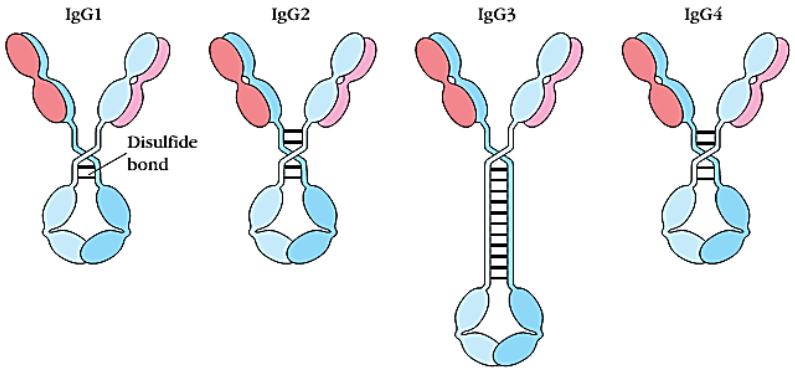

Figure 5: General structure of the subclasses of human IgG (IgG1, IgG2, IgG3, and IgG4). The main difference is related with the number and arrangement of the interchain disulfide bonds (thick black lines) that link the heavy chains. Human IgG3 has 11 interchain disulfide bonds *(14)*.

All subclasses of IgG exist in different species and their biochemical composition offers the basis for their biological functions. IgGs are smaller than the other Ig's classes, and during their isolation and purification processes, they shown to be more stable than other classes of Ig's, since they do not aggregate and they do not require the use of sugar stabilizers at pH values between

4.0 and 4.5 *(26,27)*. Furthemore, the rate of synthesis of IgG is higher than in other Ig's classes, and IgG is also highly soluble at physiological conditions *(22,26)*. IgG also displays a half-life longer than others Ig's. *(28)*. In Table 2, a summary of the main properties and characteristics of human IgG is provided.

Table 2: Main properties of human IgG *(29)*.

Properties	Immunoglobulin isotype			
	IgG1	**IgG2**	**IgG3**	**IgG4**
Heavy chain	γ_1	γ_2	γ_3	γ_4
Light chain	κ, λ	κ, λ	κ, λ	κ, λ
Other chains	-	-	-	-
Molecular weight (kDa)	146	146	170	146
Average concentration in serum ($mg \cdot mL^{-1}$)	9.0	3.0	1.0	0.5
Half-life period (days)	21	20	7	21
Total serum immunoglobulins (%)	50	17	5	3
Carbohydrates content (%)	2 – 3	2 - 3	2 – 3	2 – 3

1.3.1. Advantages and applications of IgG

Currently, the IgG isotype is one of antibodies most used in a variety of scientific, medical approaches and therapeutic applications *(30)*. These applications are a result of the higher degree of affinity and specificity of IgG for a target antigen in comparison to other antibodies *(16)*. Thus, a profound improvement on the human health can occurs by their use in diagnostic assays and therapeutics *(16)*. One of the aplications for this antibody consists on the intravenous IgG (IVIG) therapy. This therapeutic application can be applied to patients with autoimmune and inflammatory diseases (*e.g.*, Myesthenia gravis, Crohn's disease, Multiple sclerosis), as well as in patients with asthma, cardiovascular and infectious diseases *(6,31)*. Other important application of IgG is in oncology *(2)*. In this situation, the immunoglobulins act as carrier agents of toxins or radiolabeled isotopes to the cancerous cells *(30)*. In addition, these antibodies are suitable for use in indirect flow cytometry assays, for ELISA or cytotoxicity studies *(32)*.

1.3.2. Sources of IgG

Vertebrates produce five isotypes of immunoglobulins classified as IgG, IgA, IgM, IgD, and IgE *(33)*. In mammals, there are five IgG subclasses (1 to 5), which differ in effector functions *(28)*, since different IgG subclasses may be differentially produced in response to different pathogens

(34). Thus, the choice of the mammal for producing IgG is relevant because the quantity of antibody harvested depends on the animal size and robustness of their immune response *(16)*. Most polyclonal antibodies are obtained from the serum of goats or rabbits. mAbs are typically generated from rat or mouse monoclonals, yet rabbit and goat can also be used *(18)*.

In humans, as previously mentioned, there are four subisotypes of γ heavy chains corresponding to the subclasses (isotypes) IgG 1, 2, 3 and 4 *(14)*. Bovines have two subclasses of IgG, namely IgG1 and IgG2, and their concentrations in plasma are approximately the same as in humans (Table 3) *(33)*. They play a plurality of immune functions, such as the detection and elimination of invading microorganisms, for example bacteria and viruses *(33)*, and thus bovine IgG is widely used as an immunological supplement food, especially in infant formulations *(33)*. Finally, rabbits, sheep, and goats are the most commonly used mammals for producing IgG *(16)*. Among them, rabbits are the most used to generate antibodies for research because they are cheaper *(16)*, provide a large volume of immune sera *(35)*, and are highly immunogenic in responding to various immunization regimens *(34)*. Furthemore, in comparison to other species (*e.g.*, human, mouse, rat), the rabbit immune system is seemingly unique since it possesses only one IgG subclass *(28,34)*. The content of IgG in serum rabbit ranges between 13.6 $mg \cdot L^{-1}$, with a molecular weight of 143.9 kDa (heavy chains of 55 kDa and light chains between 31 and 21.5 kDa) *(34)*. Rabbit IgG antibodies are stable at high temperatures (at 70°C for 10 min are able to keep the activity without any loss) *(36)*. One important research application involving rabbit mAbs was on the HIV vaccine development, since these mAbs are able to generate long CDR3 regions, important for neutralizing the human immunodeficiency virus type 1 (HIV-1) *(34)*. A summary describing the main features amongst the Abs from different sources is described in Table 3.

Table 3: Some features that characterize Bovine, Human and Rabbit IgG, adapted from *(6,24,33,34,37)***.**

Source	Class and sub-classes	Concentration of IgG in serum /($mg \cdot mL^{-1}$)	pI
Human	IgG	10–25 (blood)	6.6
	IgG 1	5–12	8.6
	IgG 2	2–6	7.4
	IgG 3	0.5–0.1	8.3
	IgG 4	0.2–1	7.2
Bovine	IgG	40 (blood)	5.65
	IgG 1	11.2	5.6
	IgG 2	9.2	5.0
Rabbit	IgG	13.6	7.8

1.4. Methods for the purification of antibodies

In the past years, advances in science have led to a new era of therapeutic-based drugs – biopharmaceuticals *(38)*. Thus, the demand for purified proteins, such as specific antibodies, has increased considerably not only for medical use but also for advanced diagnosis *(5)*. The typical steps in antibodies (mAbs and pAbs) recovery and processing are: (i) harvest, (ii) clarification by the removal of cells and cell debris by centrifugation or microfiltration, (iii) concentration by ultrafiltration, (iv) selective purification steps, (v) virus inactivation and clearance, and (vi) validation and quality control tests *(6)* (Figure 6).

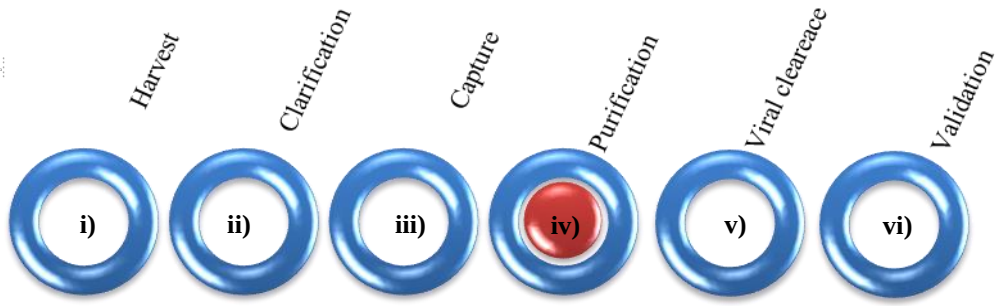

Figure 6: Typical steps involved in the production of mAbs and pAbs.

The antibodies purification (iv) is usually performed by a series of chromatographic operations, comprising the capturing, an intermediate purification (isolation), and polishing *(39)* (Figure 7).

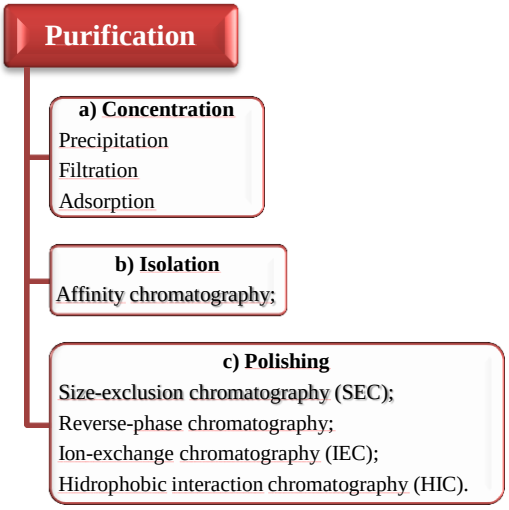

Figure 7: The steps and methods involved in the purification stage of the downstream processing of antibodies (adapted from *(26)*).

Regarding the steps of purification, the first step consists on the concentration, where the sample can be concentrated using membranes or precipitation agents, such as ammonium sulfate, polyethylene glycol or caprylic acid *(26)*; in the case of pAbs, this step consists on a precipitation induced by ethanol *(40)*. This last method consists in a separation stage by the conversion of soluble proteins to an insoluble state *(13)* that can be recovered by centrifugation and filtration *(32)*. The second step of purification includes the isolation by affinity chromatography using immobilized ligands *(26,41)*. Each type of protein has unique properties, making them specific for different target ligands *(15)*. Affinity purification procedures involve the interaction of an antibody with its antigen, generally by using binding buffers, at physiological pH and ionic strength. The antibody-ligand binding can be significantly affected by the concentration of salt in the buffer and through the impact of the ionic and dispersive interactions involved *(26)*. Biological affinity interactions are mediated by complex combinations regarding their shape, charge, hydrophobic, van der Waals and/or hydrogen bonding interactions. The highest association constant can be achieved through the identification of the type of interaction, thus selecting the buffer conditions *(26,42)*. Proteins A, G and L are the most used for the isolation of different Ig's from various mammalian species. However, the proteins and IgG interactions (Table 4) are not of the same type and strength for all animal IgGs and IgG subclasses *(14,32,42)*.

After the interaction and immobilization of the antibody by the immobilized ligand, the final step consists on the polishing attained by size exclusion chromatography (SEC). This method consists in the separation of proteins according to their size at isocratic mode. The principal trait of this technique is its non-adsorptive interaction with the sample, and even with a high retention time, there is no damage or inactivation of the proteins *(43)*. Thereby, this technique represents an important tool to remove aggregates within the antibodies purification. Nevertheless, it is not viable for large-scale applications *(6,25,44)*.

Table 4: Binding affinity for proteins A, G, and L with a variety of immunoglobulin species. w = weak binding, m = medium binding, s = strong binding, nb = no binding, – Unknown.

IgG source	Subclasses	Protein A	Protein G	Protein L
Human	IgG1	s	S	s
	IgG2	s	S	-
	IgG3	-	S	-
	IgG4	s	S	-
Rabbit	IgG	s	S	w
Bovine	IgG	w	S	nb

As explained above, the methods used for the purification of IgG involve several steps, which make the process costly and time-consuming *(38,44,45)*. Furthermore, the application of chromatographic techniques in downstream processing is limited due to their high costs, batch operation, throughput and complexity to scale up *(46)*. Thus, other alternatives for the separation and purification of proteins, particularly for therapeutic applications, have been developed with the aim of reducing costs and to be easily scaled-up, such as adsorption, ultrafiltration *(47)*, reverse micelle-mediated approaches *(48)*, and liquid-liquid extractions by means of aqueous biphasic systems (ABS) *(38)*.

1.4.1. Extraction of proteins using aqueous biphasic systems (ABS)

1.4.1.1. General concepts

Liquid-liquid extraction processes with ABS represent a viable alternative for the purification of biopharmaceuticals. An ABS consists on two immiscible aqueous-rich phases based on polymer/polymer, polymer/salt or salt/salt combinations *(7,21,45,49)*. The formation of ABS was firstly observed by Beijerinck in 1896 *(50)*. However, only in the 50s, Albertsson demonstrated their use for the isolation and separation of plant organelles and viruses *(51)*. In the past years, ABS have shown to be an alternative, efficient, and clean approach for the separation and purification of a broad array of (bio)molecules *(7,45,49)*. On the whole, both phases are composed of approximately 70-90 wt % of water, which means a biocompatible medium for biologically active molecules, constituting therefore an important advantage when the goal is to extract proteins and/or enzymes *(52)*.

The choice of the phase-forming components of ABS and their concentrations should be made taking into account the substances that need be purified and the operational requests. Salt-polymer ABS are highly recommended because these systems tend to be less viscous than polymer-polymer ABS, facilitating therefore the separation of the phases *(53)*. This type of systems has been widely exploited for the primary recovery of biological products, such as enzymes *(54)*, antibiotics *(55,56)*, antibodies *(6)*, among others *(57)*. Another advantage of these systems is the fact that the adition of salt leads to an optimization of the partitioning of the solute, typically used in the isolation and purification of biomolecules *(13)*. The basis of separation of (bio)molecules in ABS is a direct result of their selective distribution between the two distinct aqueous phases *(58)*. However, a high extractive performance can be achieved by the manipulation of the affinity of the target compound for each of the aqueous-rich phases. Even so, traditional polymer-salt and salt-salt systems display a restricted polarity at the coexisting phases

which have limited their successful application to the purification (selective extraction) of target and added-value products, such as biopharmaceuticals *(3,59)*. To overcome this drawback, ILs have been introduced as phase-forming components of ABS leading to a high extraction performance *(9)*, and as will be discussed below in more detail.

For the design of ABS as extraction and purification processes, their phase diagrams and respective tie-lines are required. All ABS have a unique phase diagram under a particular set of conditions, such as temperature and pH *(52,57)*. Thus, before any application, it is extremely important to determine the respective phase diagram for a particular pair of phase-forming components aiming at gathering the information necessary on the monophasic/biphasic regimes before any extraction/purification procedure. In addition, the determination of the corresponding tie-lines (TLs) gives the equilibrium composition of the top and bottom phases *(60–62)*. Figure 8 depicts an example of a phase digram of an ABS composed of a polymer (polyethylene glycol, PEG), a salt and water, and the binodal curve. The binodal curve, TCB, represents the separation between the miscible and immiscible regions, i.e., above the binodal curve it is located the biphasic region, while below it is the single phase region *(60,62)*. The larger the biphasic region, the higher the ability of the phase-forming components to undergo liquid-liquid demixing. Three mixture compositions at the biphasic region are also identified as X, Y and Z in Figure 8. The mixtures X, Y and Z are along the same tie-line (TL) meaning that all the initial mixtures will present the same top (T_{PEG}, T_{Salt}) and bottom phase compositions (B_{PEG}, B_{Salt}) *(63)*.

The TLL is a numerical indicator of the composition difference between the two phases and is often used to correlate with the trends observed in the partitioning of solutes between the phases *(3)*.

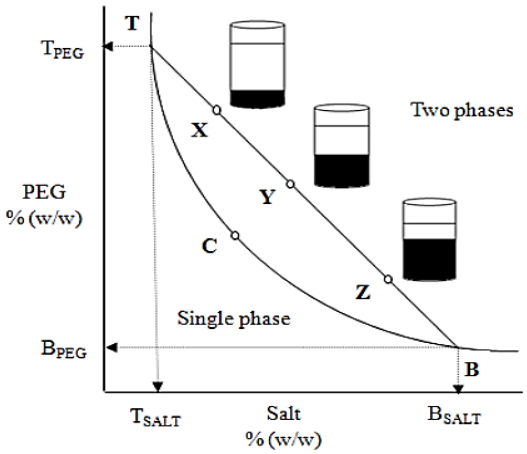

Figure 8: Schematic representation of a phase diagram of an ABS. TCB - Binodal curve, C - Critical point, TB - Tie-line, T - composition of the top phase, B - composition of the bottom phase; and X, Y and Z - total composition of biphasic mixtures *(62)*.

1.4.1.2. ABS as an alternative to conventional methods

Conventional biotechnological processes usually require numerous steps with high energy and chemical consumptions, representing about 60-90% of the cost of the final product *(5)*. ABS, due to their advantages, are a potential alternative to the traditional technologies for the recovery and purification of biomolecules *(5)*.

The pratical strategies for the design of an appropriate recovery process using ABS can be divided into four stages, namely the initial physicochemical characterization of the feedstock – product and major contaminants molecular weight, isoelectric point, hydrophobic character, etc; selection of the type of ABS; selection of the system parameters; and evaluation of the influence of the process parameters upon the product recovery/purity *(57)* (Figure 9).

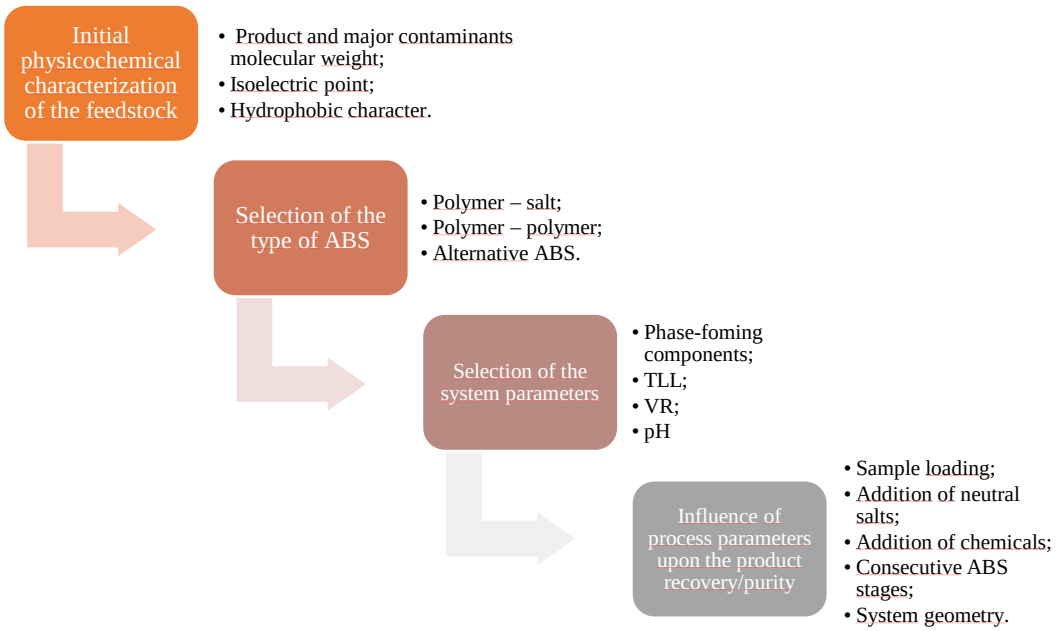

Figure 9: Simplified representation of the strategies for the design of the recovery of biological products using ABS (adapted from *(57)*).

ABS are favourable for the extraction of proteins due to the high amount of water present in the phases *(2,5,7)*. Moreover, these systems are of lower cost when compared with chromatographic strategies, are more environmentatlly benign since the use of volatile organic compounds is avoided, allow the scale-up and lead to high extraction performance and purity levels. For instance, a comparison between a purification process using ion-exchange chromatography, with a previous acetone fractionation, and an ABS extraction, demonstrated superior overall recovery of the enzyme α-galactosidase in ABS (11.5 *vs.* 87.6%, respectively) *(64)*. Other widely used technique for the purification of proteins/enzymes consists on the precipitation of the target molecule with ammonium sulfate. A comparison between the two methods was already performed and ABS exceeded the precipitation method, achieving a greater recovery yield (88 % *vs.* 49 %) and purity (100 % *vs*. 89 %) of papain from wet *Carica papaya* latex *(65)*. It is thus clear that ABS can serve as an alternative method over other conventional separation processes, and in particular for proteins and enzymes, and so, these systems have been subject of an increased attention and research.

1.4.1.3. Extraction and purification of IgG using ABS

The first report describing the use of polymer/salt ABS for the purification of both monoclonal and polyclonal antibodies from different feedstocks dates from 1992, by Sulk *et al.*

(66) using PEG/phosphate-based salts systems. Later on, Zijlstra and co-workers *(67)* synthesized a functionalised PEG to combine with dextran and to form ABS, aiming at recovering IgG from hybridoma cells. Moreover Asenjo *et al*. *(68)* used an ABS composed of PEG, a phosphate-based salt and NaCl to successfully recover IgG from hybridoma cell supernatants in the top phase. In the same line, Rito-Palomares *et al. (69)* studied PEG-potassium phosphate ABS to process whole bovine blood, resulting in the partition of bovine serum albumin (BSA), haemoglobin and IgG into the PEG-rich phase and cell debris into the phosphate-rich bottom phase. A partition coefficient for IgG of 55 was attained *(69)*. Finally, *Aires-Barros and co-workers (2–4,6,7,20,21,44,49,70,71)* devoted a large attention on the study of ABS for the purification of IgG. A list of the systems, phase-forming components and conditions investigated are summarized in Table 5. It should be highlighted that all these investigations were carried out with CHO and hybridoma cell supernatants, and thus with monoclonal IgG.

Table 5: List of different ABS used to purify and recover monoclonal IgG.

ABS % (w/w)	pH	Recovery yield (%)	Ref.
[PEG 3350 + Potassium Phosphate] + NaCl	6	89	*(71)*
[PEG 3350 + Potassium Phosphate] + NaCl	6	97	*(6)*
[PEG 6000 + Potassium Phosphate] + NaCl	6	88	*(3)*
[PEG 3350 + Potassium Phosphate] + NaCl	6	80	*(4)*
[PEG 3350 + Sodium Citrate]	6	97	*(70)*
[PEG 3350 + Sodium Citrate] + NaCl	6	99	*(21)*
[PEG 3350 + Dextran 500 kDa] + Diglutaric acid	7	97	*(49)*
[PEG 3350 + Dextran 500 kDa]	7	95	*(20)*
[PEG 6000 + Dextran 500 kDa] + NaCl	3	87	*(2)*

In some studies *(3,4,6,71)*, several ABS for the extraction and purification of IgG from a mixture of proteins or Chinese hamster ovary (CHO) cells supernatant were investigated. The authors observed that the NaCl and the phosphate-based salt concentrations are the factors that display the most significant influence on the amount of native IgG present at the top phase *(3)*. When the PEG concentration is increased, a decrease on the partition coefficient and extraction yield of IgG for the top phase was observerd *(3,6)*. Considering a two-step extraction an IgG total yield of 76% and a purity of 100% were obtained *(6)*. Therefore, the authors proposed a multi-stage equilibrium aqueous two-phase extraction for the successful purification of human antibodies from a CHO cells supernatant *(4,6,71)*.

The viability of using multi-stage extractions, as an important tool for the removal of contaminants in the downstream processing of human antibodies, was also shown by Rosa *et al. (20)* with polymer-polymer ABS. In an adiditonal study *(70)*, the authors demonstrated the feasibility of combining the extraction carried out by ABS with HIC (Hydrophobic interaction chromatography) and SEC (Size exclusion chromatography) for the purification of human therapeutic antibodies without the use of any conditioning step in the three unit operations. ABS composed of 10% (w/w) of PEG 3350 and 12% (w/w) of sodium citrate, followed by a phenyl-sepharose HIC column and SEC led to the acquisition of 100% pure IgG with a 90% yield.

The partitioning and purification of antibodies was also enhanced using functionalised-PEG polymers as phase-forming components of ABS *(49)*. An ABS composed of 5% dextran, 8% of PEG diglutaric acid and 10 mM phosphate buffer at pH 7, allowed the extraction of 97% of IgG to the top phase, with a purity of 94% *(49)*. In 2007, Hye-Mee Park *et al. (72)* suggested a novel affinity separation method, where horseradish peroxidase (HRP) and human IgG were used as a ligand carrier and an affinity ligand, respectively. They tested two different ABS, one consisting of potassium phosphate (15%, w/w) and PEG 1450 (10%, w/w) and the other composed of dextran 500 kDa (5% w/w) and PEG 8000 (5% w/w). The authors *(72)* observed that conjugated human IgG-HRP preferentially migrates for the PEG-rich top phase, whereas human IgG, rabbit anti-human IgG and goat anti-mouse IgG preferred the salt or dextran-rich bottom phase. The best results were obtained with the dextran-based ABS where the yield and purity of the recovered rabbit anti-human IgG were 90.8 and 87.7%, respectively *(72)*.

Vargas and co-workers *(73)* developed a new and cost-effective plasma fractionation method using an ABS composed of PEG 3350, potassium phosphate and sodium chloride, at pH 6.1, for IgG from human plasma collected from Costa Rican healthy donors. At the best conditions evaluated, IgG precipitated in the PEG-rich upper phase (83% recovery), and after polishing, IgG was obtained at a recovery of 70% and with a purity of 92% *(73)*. Wu et al. *(74)* used PEG 4000, hydroxypropyl starch (HPS) and NaCl at pH 8.0 to extract IgG from human serum albumin. The results obtained displayed a IgG recovery in the PEG-rich phase with 99.2% of extraction yield *(74)*.

Polymer-polymer ABS have been largely investigated for the purification of IgG *(2,7,20,44,49,74–76)*. However, these systems display high viscosities at the coexisting phases *(38)*. Furthermore, dextran is too expensive as a phase-forming component to scale-up the extraction process *(77)*. To overcome these drawbacks, most works in literature describe the use of polymer–salt systems *(3,4,6,21,69–73,78,79)* thereby decreasing the viscosity of the coexisting

phases, providing a higher density difference, and thus faster separation rates, as well as by providing lower cost systems and their scale-up *(38,80)*. These systems are mainly composed of inorganic salts, especially phosphate-based *(21,38)*, and some biodegradable organic salts, such as sodium citrate *(8,80)*.

One of the most used polymers in ABS is PEG (Figure 10). PEG is a polyether diol with two terminal hydroxyl groups, which can be exposed to chemical derivatization. Polymers offer some degree of design, for instance, by varying the length of the polymeric chains, *i.e.*, by changing their average molecular weight, or by changing the structure of the monomer unit. PEG also displays some attractive properties, such as biodegradability, low toxicity, low volatility, low melting points, high water solubility and low cost *(9)*. However, the hydrophilic nature of PEG limits the applicability of this technique when the goal is to extract hydrophobic biomolecules. To overcome this limitation, recent works have introduced ionic liquids (ILs) to tune the properties of PEG through the modification of its chemical structure and thus increasing the extraction yield *(9)*, as well as by using ILs as adjuvants in traditional polymer-salt or polymer-polymer ABS *(9,81–84)*.

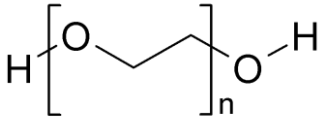

Figure 10: Chemical structure of PEG with the molecular formula H-(O-CH_2-CH_2)$_n$-OH.

1.5. Ionic liquids as novel and alternative strategies in polymer-salt-based ABS

Ionic liquids (ILs) are organic salts with melting points below 100 °C *(85)*. They are usually constituted by a large and organic cation and an organic or inorganic anion *(22)*. The low melting temperatures of ILs are typically associated with the lack of an ordered crystalline structure *(22)*. Amongst the large range of ILs that can be synthesized, the most commonly studied are nitrogen-based, with their general cation structures presented in Figure 11 *(86–89)*.

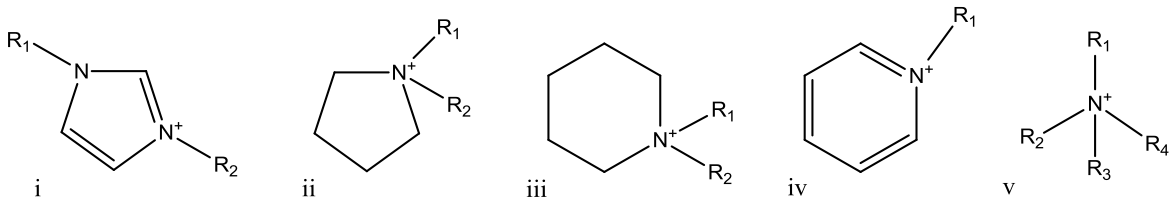

Figure 11: Cation structures of nitrogen-based ILs: (i) dialkylimidazolium, (ii) dialkylpyrrolidinium, (iii) dialkylpiperidinium, (iv) alkylpyridinium and (v) tetralkylammonium.

The first IL synthesized was ethylammonium nitrate, in 1914, by Paul Walden *(26)*. Later, in 1934, Charles Graenacher filled the first patent regarding an industrial application of ILs in the preparation of cellulose solutions *(27)*. During the 2nd World War, new patents involving the use of ILs have appeared, while contemplating mixtures of aluminium chloride (III) and 1-ethylpyridinium bromide for the electrodeposition of aluminium *(28,29)*. Despite these findings, only more recently, in 1992, air and water stable ILs were synthetized *(30)*.

ILs are a group of "green solvents" with attractive properties, namely a negligible volatility and non-flammability, under ambient conditions, which contributed to this characterization *(63,90–92)*. Other important properties include a high chemical/thermal stability, a wide electrochemical window, a strong solubility power and a large number of possible variations in the cation and anion which further allow the fine-tuning of these properties *(63,90,91)*.

Many researchers have reported the capacity of enzymes and proteins to remain stable and active in presence of IL aqueous solutions *(91,93)*. The first attempt on the direct extraction of proteins using ABS composed of ILs was reported by Wang *et al. (94)* using and ABS formed by the hydrophilic IL 1-butyl-3-methylimidazolium chloride ($[C_4mim]Cl$) and K_2HPO_4. No chemical (bonding) interactions between proteins and the IL ions were observed during the extraction process, as well as no alterations on the native conformation of proteins. In the same line, other recent works demonstrated the extraction performance and the stability of proteins using IL-based ABS *(93,95–97)*.

Cheng *et al*. *(98,99)* evaluated a large series of hydrophobic ILs for the extraction of heme-proteins, namely hemoglobin and cytochrome-c. Regarding the extraction of antibodies with IL-based systems, two works were found in the literature. Martínez-Aragón *et al. (5)* tried to purify IgG monoclonal antibodies from their fermentation broth with three ILs immiscible with water, namely tetradecyl(trihexyl)phosphonium bistriflamide, $[P_{14,6,6,6}][NTf_2]$, tetradecyl(trihexyl) phosphonium dicyanamide, $[P_{14,6,6,6}][N(CN)_2]$, and 1-ethyl-3-methylimidazolium bis[(trisfluoromethyl)sulfonyl] amide, $[C_2mim][NTf_2]$. They concluded that IgG does not suffers precipitation with $[P_{14,6,6,6}][N(CN_2)]$, $[P_{14,6,6,6}][NTf_2]$ and $[C_2mim][NTf_2]$ *(5)*. The stability of IgG1 was also tested into two ILs, namely Iolilyte 221 PG (an ammonium-based IL with an oligopropyleneglycol unit at the side chain) and tributylmethylphosphonium methylsulfate ($[P_{4,4,4,1}][CH_3SO_4]$). At 10% w/w of ILs, the authors did not observe the IgG fragmentation or agregation; however, IgG1 formed aggregates at higher concentrations of Iolilyte 221 PG *(100)*.

1.5.1. ILs as adjuvants in polymer-salt- based ABS

Besides the introduction of ILs to functionalize PEG *(101)*, in others works, small quantities of ILs (as adjuvants) were added into conventional polymer-salt-ABS to tailor the extraction and selectivity performances *(9,81–84)*. As already mentioned, the hydrophilic nature of PEG limits the applicability of the ABS technique, specially, when the goal is to extract hydrophobic (bio)molecules *(9,81,83,84,102)*, like IgG. For example, Pereira *et al. (9)* investigated the potential of using ILs as adjuvants (at 5 wt%) in typical PEG/inorganic salt ABS for the separation and purification of model biomolecules (L-tryptophan was used as an essential amino acid model). In general, the results showed that salting-in inducing ILs enhance the partition coefficient of L-tryptophan for the PEG-rich phase while salting-out inducing ILs decrease the partitioning of the amino acid. In the same line, Hamzehzadeh *et al. (84)* investigated the potential of the IL 1-butyl-3-methylimidazolium bromide ($[C_4mim]Br$) as an adjuvant in ABS formed by PEG 400 + tri-potassium citrate ($K_3C_6H_5O_7$), on the separation of L-tryptophan. It was possible to demonstrate that the presence of small quantities of $[C_4mim]Br$ enhances up to twice the extraction ability of the amino acid for the polymer-rich phase. In a similar work *(83)*, the influence of the addition of 5 wt% of $[C_4mim]Br$ to ABS formed by PEG 600 + $K_3C_6H_5O_7$ was evaluated for the extraction of L-tyrosine (Tyr).

Furthermore, Almeida *et al*. *(102)* proposed ABS composed of PEG, Na_2SO_4 and ILs (at 5 or 10 wt%) as an alternative technique for the extraction, separation and/or purification of gallic, vanillic and syringic acids. The results obtained clearly demonstrated the ability of ILs to tune the

polarity of the PEG-rich phase and to tailor the extraction of phenolic acids. Furthermore, de Souza *et al. (81)* investigated the impact of several imidazolium-based ILs as adjuvants in the formation of ABS constituted by potassium salts, water and PEG (1500, 4000, 6000 and 8000). The ILs influence was also evaluated on the partition behavior of Chloranilic Acid and Rhodamine 6G *(81)*. Moreover, the same approach was used by Souza *et al. (82)* in which imidazolium-based ILs as adjuvants in polymer-salt ABS were used to purify an enzyme.

Taking into account the previous works *(9,81–84,102)*, it is possible to conclude that the use of ILs as adjuvants to modify the characteristics of the polymer-rich phase could be an interesting alternative in separation processes and opens the door for a new range of IL-based extraction processes.

Considering the advantages described before in the use of polymer-salt-based ABS for the recovery/purification of IgG, combined with the tailoring ability afforded by ILs, the aim of this work consists on the use of ILs as adjuvants in PEG-salt ABS for the separation and purification of IgG from rabbit serum.

2. Experimental section

2.1. Chemicals

In this work, PEGs with different molecular weights, namely 400, 600, 1000, 2000, 4000 and 8000 g·mol^{-1} (herein abbreviated as PEG 400, PEG 600, PEG 1000, PEG 2000, PEG 4000 and PEG 8000, respectively) were studied. They were obtained from Sigma–Aldrich, with the exception of PEG 1000 that was obtained from Fluka The salts used were the potassium citrate tribasic monohydrate ($K_3C_6H_5O_7 \cdot H_2O$, purity ≥ 99 wt%), acquired from Sigma–Aldrich Chemical Co. (USA), and citric acid monohydrate, $C_6H_8O_7.H_2O$, from Panreac (EU).

The water employed was double distilled, passed across a reverse osmosis system and further treated with a Milli-Q plus 185 water purification apparatus.

IgG from rabbit serum (reagent grade, ≥ 95%) as a lyophilized powder, 113.6 mg of solid, was purchased from Sigma-Aldrich.

In this work different ILs were investigated, namely: 1-butyl-3-methylimidazolium bromide, [C_4mim]Br (purity of 99 wt %); 1-ethyl-3-methylimidazolium chloride, [C_2mim]Cl (purity of 99 wt %); 1-butyl-3-methylimidazolium chloride, [C_4mim]Cl (purity of 99 wt %); 1-hexyl-3-methylimidazolium chloride, [C_6mim]Cl (purity of 99 wt %); 1-octyl-3-methylimidazolium chloride, [C_8mim]Cl (purity of 99 wt %); 1-decyl-3-methylimidazolium chloride, [C_{10}mim]Cl (purity of 99 wt %); 1-dodecyl-3-methylimidazolium chloride, [C_{12}mim]Cl (purity of 99 wt %); 1-tetradecyl-3-methylimidazolium chloride, [C_{14}mim]Cl (purity of 99 wt %); 1-butyl-3-methylimidazolium tosylate, [C_4mim][Tos] (purity of 98 wt %); 1-butyl-3-methylimidazolium dicyanamide, [C_4mim][$N(CN)_2$] (purity > 98 wt %); and 1-butyl-3-methylimidazolium acetate, [C_4mim][CH_3CO_2]. The chemical structures of the investigated ILs are depicted in Figure 12. All ILs were purchased from Iolitec. Before use, all ILs were purified and dried for a minimum of 24 h, under constant agitation, at moderate temperature (≈ 353 K) and under vacuum (to reduce their volatile impurities to negligible values). After this step, the purity of each IL was also confirmed by ^{1}H and ^{13}C NMR spectra and found to be in accordance with the purity levels given by the supplier.

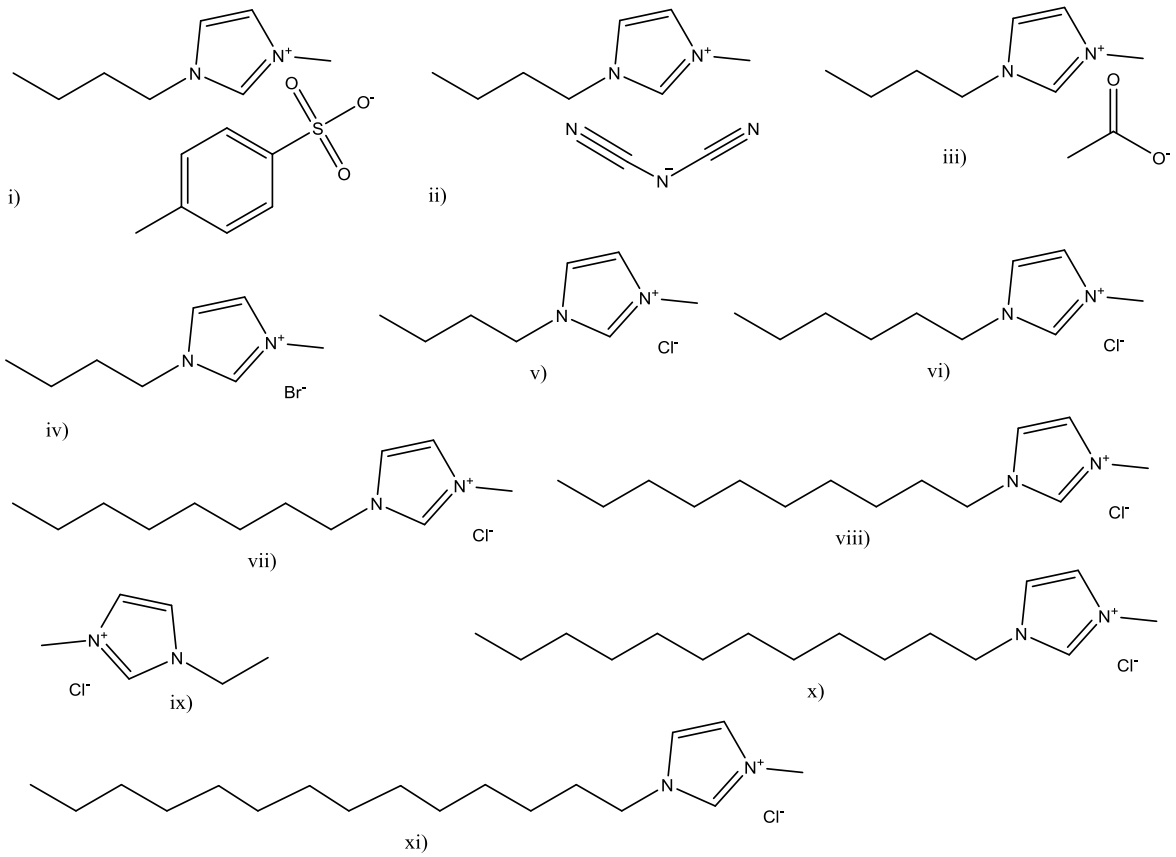

Figure 12: Chemical structures of the ILs investigated: (i) [C_4mim][Tos]; (ii) [C_4mim][$N(CN)_2$]; (iii) [C_4mim][CH_3COO]; (iv) [C_4mim][Br]; (v) [C_4mim][Cl]; (vi) [C_6mim][Cl]; (vii) [C_8mim][Cl]; (viii) [C_{10}mim][Cl]; (ix) [C_2mim][Cl]; (x) [C_{12}mim][Cl]; (xi) [C_{14}mim][Cl].

2.2. Experimental procedure

2.2.1. Phase diagrams, tie-lines (TLs) and critical point

Phase diagrams comprise a binodal curve and different tie-lines (TLs). While the binodal curve represents the borderline between the monophasic region and the biphasic region, the TL describes the compositions of the two phases in equilibrium for given mixture compositions. The respective ternary phase diagrams were determined for each of the water-soluble PEGs (PEG 200, PEG 400, PEG 600, PEG 1000, PEG 2000, PEG 4000, PEG 6000 and PEG 8000) at pH ≈ 7 and for PEG 400 in the range from pH 5 to 9. The buffer solutions ($K_3C_6H_5O_7/C_6H_8O_7$) mixtures were used to maintain the pH of the overall ABS at the desired value. The binodal curve of each ABS was determined through the cloud point titration method at 25 ^oC and atmospheric pressure *(21)*, using aqueous solution of salt at around 50 wt % and aqueous solutions of the different hydrophilic PEGs (with concentrations ranging from 60 wt % to 90 wt %). The experimental

procedure has been validated in previous reports *(103,104)*. Repetitive drop-wise addition of the aqueous salt solution to the polymer solution, or *vice-versa*, was carried out until the detection of a cloudy solution (biphasic region), followed by the drop-wise addition of ultra-pure water until the detection of a clear and limpid solution (monophasic region). This procedure was carried under constant stirring. Each mixture composition was determined by the weight quantification of all components added within an uncertainty of ± 10^{-4} g (using an analytical balance, Mettler Toledo Excellence XS205 DualRange).

The TLs of each phase diagram were determined by a gravimetric method originally described by Merchuk et al. *(105)*. A mixture at the biphasic region was gravimetrically prepared (PEG + Salt + water) within ± 10^{-4} g, vigorously stirred, and left for at least 12 h at 25 °C to reach the complete separation and equilibration of the coexisting phases. After the separation step, both top and bottom phases were weighted.

The experimental binodal curves were fitted using Equation (1) *(105)*:

$$[PEG] = A\exp[(B[salt]^{0.5}) - (C[salt]^3)] \quad (1)$$

where $[PEG]$ and $[salt]$ are, respectively, the PEG and salt weight percentages and A, B and C are constants obtained by the regression.

Each individual TL was determined by the application of the lever-arm rule to the relationship between the top phase weight and the overall system composition. For the determination of TLs it was solved the following system of four equations (Equations 2 to 5) and four unknown values ($[PEG]_{\mathrm{PEG}}$, $[PEG]_{\mathrm{salt}}$, $[salt]_{\mathrm{PEG}}$ and $[salt]_{\mathrm{salt}}$) *(105)*:

$$[PEG]_{\mathrm{PEG}} = A\exp\left[\left(B[salt]_{\mathrm{PEG}}^{0.5}\right) - \left(C[salt]_{\mathrm{PEG}}^{3}\right)\right] \quad (2)$$

$$[PEG]_{\mathrm{salt}} = A\exp\left[\left(B[salt]_{\mathrm{salt}}^{0.5}\right) - \left(\mathrm{C}[salt]_{\mathrm{salt}}^{3}\right)\right] \quad (3)$$

$$[PEG]_{\mathrm{PEG}} = \frac{[PEG]_{\mathrm{M}}}{\alpha} - \left(\frac{1-\alpha}{\alpha}\right)[PEG]_{\mathrm{salt}} \quad (4)$$

$$[salt]_{\mathrm{PEG}} = \frac{[salt]_{\mathrm{M}}}{\alpha} - \left(\frac{1-\alpha}{\alpha}\right)[salt]_{\mathrm{salt}} \quad (5)$$

The subscripts PEG, salt and M represent the top, bottom and the mixture phases, respectively. The parameter α is the ratio between the PEG-rich phase weight and the total weight of the two phases. The solution of the referred system gives the concentration (wt %) of the PEG and salt in the top and bottom phases, and thus TLs can be easily represented.

For the calculation of the tie-line lengths (TLLs) it was applied Equation. (6).

$$TLL = \sqrt{([salt]_{\mathrm{PEG}} - [salt]_{\mathrm{salt}})^2 + ([PEG]_{\mathrm{PEG}} - [PEG]_{\mathrm{salt}})^2} \quad (6)$$

The critical point of each ABS was determined by extrapolating the TLs' slopes of individual systems by the fitting provided by Equation (7),

$$[\mathrm{Salt}] = f[\mathrm{PEG}] + g \quad (7)$$

where *f* and *g* are fitting parameters.

2.2.2. pH measurements

The pH values of both the PEG-rich and organic-salt-rich aqueous phases were measured at (25 ± 1) ºC using a METTLER TOLEDO SevenMulti pH meter within an uncertainty of ± 0.02.

2.2.3. Extraction of IgG using PEG-salt based ABS

The ternary mixture compositions for the IgG extraction were chosen based on the phase diagrams determined for each PEG-$C_6H_5K_3O_7$/$C_6H_8O_7$. Moreover, to avoid discrepancies in the results which could arise from the different compositions between the two phases, all the partitioning studies were performed at a constant TLL. The mixture compositions which correspond to a TLL of 35 are as follows: 25 wt% of PEG 400 + 25 wt% of $C_6H_5K_3O_7$/$C_6H_8O_7$, 19 wt% of PEG 600 + 23 wt% of $C_6H_5K_3O_7$/$C_6H_8O_7$, 19 wt% of PEG 1000 + 20 wt% of $C_6H_5K_3O_7$/$C_6H_8O_7$, 18 wt% of PEG 2000 + 16 wt% of $C_6H_5K_3O_7$/$C_6H_8O_7$, 18 wt% of PEG 4000 + 14 wt % of $C_6H_5K_3O_7$/$C_6H_8O_7$, 17 wt% of PEG 6000 + 14 wt % of $C_6H_5K_3O_7$/$C_6H_8O_7$, and 16 wt% of PEG 8000 + 15 wt % of $C_6H_5K_3O_7$/$C_6H_8O_7$. The partition behaviour of rabbit IgG in aqueous PEG/citrate buffer two-phase systems was investigated using IgG stock solutions prepared with a concentration at *circa* 1 $g{\cdot}L^{-1}$ dissolved in PBS (phosphate buffered saline at 0.01M and pH ≈ 7.4 at 25ºC). In each

system, a small amount of the solution containing IgG (≈ 0.30 mg) was added to the phase-forming components to reach a total weight of the mixture of 1.5 g.

In order to elucidate the main factors that rule the partition behavior of IgG in polymer/salt ABS, three main parameters were investigated.

Effect of equilibrium time

Firstly, it was studied the effect of the extraction time. For this purpose, the polymers with the highest (PEG 8000) and the lowest (PEG 400) molecular weight were used. The mixtures were prepared at pH ≈ 7, same of them were submitted at 10 min by centrifugation at 1000 rpm (VWR, Micro Star 17), followed by different times of equilibrium, namely 10, 30, 60, 90 and 120 min of rest, while others were left to phase separate (with no centrifugation) for 300 and 720 min at 25 °C. ABS composed PEG 400, PEG 8000 and PEG 2000, at pH ≈ 7, were also submitted to centrifugation for 10 min at 1000 rpm followed by 60, 120 and 180 min of rest at 25° C.

Effect of molecular weight of PEG

The second parameter studied was the PEG molecular weight (namely, 400, 600, 1000, 2000. 4000, 6000, 8000 $g \cdot mol^{-1}$). In this study, mixtures at pH ≈ 7 were prepared and centrifuged for 10 min, at 1000 rpm, and left to equilibrate for 120 min at 25^{o}C to ensure the total phases separation.

Effect of pH

The last parameter comprises the study of the effect of pH through the IgG extraction. In this case, mixtures at different pH values (6, 8, and 9) were prepared, centrifuged at 1000 rpm for 10 min and left to equilibrate for more 120 min at 25 °C, to ensure total phase separation. In this part, the mixture compositions which correspond to a TLL of 35 are as follows: 19.88 wt% of PEG 400 + 35.40 wt% of $C_6H_5K_3O_7/C_6H_8O_7$, at pH ≈ 5; 21.92 wt% of PEG 400 + 29.37 wt % of $C_6H_5K_3O_7/C_6H_8O_7$, at pH ≈ 6; 21.42 wt% of PEG 400 + 25.67 wt % of $C_6H_5K_3O_7/C_6H_8O_7$, at pH ≈ 8; and 23 wt% of PEG 400 + 25 wt % of $C_6H_5K_3O_7/C_6H_8O_7$, at pH ≈ 9.

In the studied ABS, the top phase corresponds to the PEG-rich aqueous phase, while the bottom phase is mainly composed of salt. After a careful separation of both phases, the quantification of IgG in the two phases was carried by UV-spectroscopy, using a UV-spectrophotometry (SYNERGY|HT microplate reader, BioTek), at a wavelength of 280 nm, using calibration curves previously established (cf. Appendix A - Figure A.1). At least three individual

experiments were performed in order to determine the average in the partition coefficient, extraction efficiency and extraction yields, as well as, the respective standard deviations. The interference of the salt and PEG with the quantification method was also ascertained and blank control samples were always used.

The partition coefficient of the studied rabbit IgG, K_{IgG}, is defined as the ratio of the concentration of IgG in the PEG-rich to that in the salt-rich aqueous phase according to Equation (8),

$$K_{\mathrm{IgG}} = \frac{[\mathrm{IgG}]_{\mathrm{PEG}}}{[\mathrm{IgG}]_{\mathrm{Salt}}} \quad (8)$$

The percentage extraction efficiency of IgG into to PEG-rich phase, $EE_{\mathrm{IgG}}\%$, is the percentage ratio between the amount of protein in the PEG-rich aqueous phase to that in the total mixture, and is defined according to Equation (9),

$$EE_{\mathrm{IgG}}\% = \frac{w_{IgG}^{PEG}}{w_{IgG}^{PEG} + w_{IgG}^{Salt}} \times 100 \quad (9)$$

where w_{IgG}^{PEG} and w_{IgG}^{Salt} are the weight of IgG in the PEG-rich phase and in the salt-rich phase, respectively.

The extraction yield of IgG into to PEG-rich phase, $Y_{\mathrm{IgG}}\%$, is the percentage ratio between the amount of protein in the PEG-rich aqueous phase to that added in the initial mixture ($w_{IgG}^{Initial}$), and is defined according to Equation (10).

$$Y_{\mathrm{IgG}}\% = \frac{w_{IgG}^{PEG}}{w_{IgG}^{Initial}} \times 100 \quad (10)$$

2.2.4. Extraction of IgG using ILs as adjuvants in PEG-salt based ABS

After the previously described optimisation procedures, a mixture point, with a composition of 25 wt% of PEG 400 + 25 wt% of $C_6H_5K_3O_7$/$C_6H_8O_7$ at pH ≈ 7 (TLL of 35) was selected. In this mixture, 5 wt% of each IL was added, and the partition behaviour of rabbit IgG was investigated. The ILs used for the study of the anion effect were: [C_4mim]Br; [C_4mim]Cl [C_4mim][Tos]; [C_4mim][$N(CN)_2$]; [C_4mim][CH_3CO_2]; while to study the effect of the cation nature the following ILs were employed: [C_2mim]Cl, [C_4mim]Cl, [C_6mim]Cl, [C_8mim]Cl, [C_{10}mim]Cl, [C_{12}mim]Cl, and [C_{14}mim]Cl. The stock solutions were prepared with a concentration at *circa* 1 $g{\cdot}L^{-1}$ of rabbit serum IgG, dissolved in PBS (phosphate buffered saline at 0.01M, pH ≈ 7.4). In each system, a small

amount of solution content IgG (≈ 0.30 mg) was added to a total weight of 1.5 g corresponding to the ABS. Each mixture was then stirred, centrifuged for 10 min, at 1000 rpm, at 25ºC, and left to equilibrate for more 120 min (a time period established in the previous optimization experiments) in order to achieve the complete partitioning of IgG between the two phases. Again, the PEG-rich phase is the top layer, while the salt-rich phase corresponds to the bottom layer.

After a careful phase separation, the top phase sample was diluted. Subsequently, $K_{\mathrm{IgG}}\%$ was assessed using equation (8), $EE_{\mathrm{IgG}}\%$ was determined using equation (9) and $Y_{\mathrm{IgG}}\%$ was determined using equation (10). These parameters were evaluated using data obtained by UV-spectroscopy, using a (SYNERGY|HT microplate reader, BioTek), at a wavelength of 280 nm. Furthermore, the partition coefficient of the IL, K_{IL}, is defined as the ratio of the IL in the PEG-rich to that in the salt-rich aqueous phase according to Equation (11),

$$K_{\mathrm{IL}} = \frac{\mathrm{Abs}_{\mathrm{IL}}^{PEG}}{\mathrm{Abs}_{IL}^{Salt}} \qquad (11)$$

where $\mathrm{Abs}_{\mathrm{IL}}^{\mathrm{PEG}}$ and $\mathrm{Abs}_{\mathrm{IL}}^{\mathrm{Salt}}$ are the absorbance of IL at the maximum wavelength (211 nm), adjusted by the respective dilution factor, in the PEG-rich and in the salt-rich aqueous phases, respectively.

3. Results and discussion

3.1. Phase diagrams, tie-lines (TLs) and critical point

3.1.1. Effect of the molecular weight of PEG

The development of more efficient, economic and environmentally-friendly processes to extract and purify biopharmaceuticals, while envisaging their large scale applications, is a vital requirement. Thus, in this work, polymer-organic-salt-based ABS, as well as ABS employing ILs as adjuvants, were used to evaluate their extraction ability for IgG before moving to real serum samples. The organic salt and the polymers used are of low cost, biodegradable and non-toxic compounds *(7,8)*.

The ternary phase diagrams were determined at 25 ^{o}C for several PEGs with different molecular weights (PEG 200, 400, 600, 1000, 2000, 4000, 6000 and 8000) and the citrate buffer at pH ≈7 in aqueous medium. The phase diagrams obtained are illustrated in Figure 13 (the experimental weight fraction data of each phase diagram are given at Appendix B, Table B. 1 to Table B. 4). The respective phase diagrams in molality units are presented in Appendix C, in Figure C. 1. For all the studied ABS, the top phase corresponds to the aqueous PEG-rich phase while the bottom phase is mainly composed of $C_6H_5K_3O_7$/$C_6H_8O_7$ and water. The results for PEG 200 are not showed, since after several experimental attempts, it was found that there is no formation of a biphasic system between PEG 200 and $C_6H_5K_3O_7$/$C_6H_8O_7$ at pH ≈ 7.

By plotting each phase diagram (Figure 13), it is possible to realize the influence of the length of the PEG chains on the phase diagram behavior, and on the PEG ability to create ABS. In all phase diagrams, the biphasic region is localized above the solubility curve, and larger this region is, the higher is the ability of PEG to undergo liquid-liquid demixing in the presence of $C_6H_5K_3O_7$/$C_6H_8O_7$ at pH ≈7. In general, for polymers of lower molecular weight the phase separation only occurs at higher concentrations of PEG. Thus, with the increase of the PEG molecular weight, it increases their ability to form ABS systems, and in the following order: PEG 400 < PEG 600 < PEG 1000 <PEG 2000 < PEG 4000 < PEG 6000 < PEG 8000. Similar trends have been observed in other ABS composed of polymer/salt or PEG/IL pairs *(21,102,106,107)*. This behavior is a consequence of the higher hydrophobicity displayed by PEGs of higher molecular weight*, i.e.,* they present a lower affinity for water, and are more easily excluded for a second liquid phase by the salting-out species ($C_6H_5K_3O_7$/$C_6H_8O_7$). The systems composed of PEG 1000, 2000, 4000 and 6000 and potassium citrate and water have been reported in the literature being

the results obtained in close agreement with literature data *(107)* - Appendix C, Figure C. 2. Nevertheless, for PEGs of lower molecular weight novel experimental data are here shown.

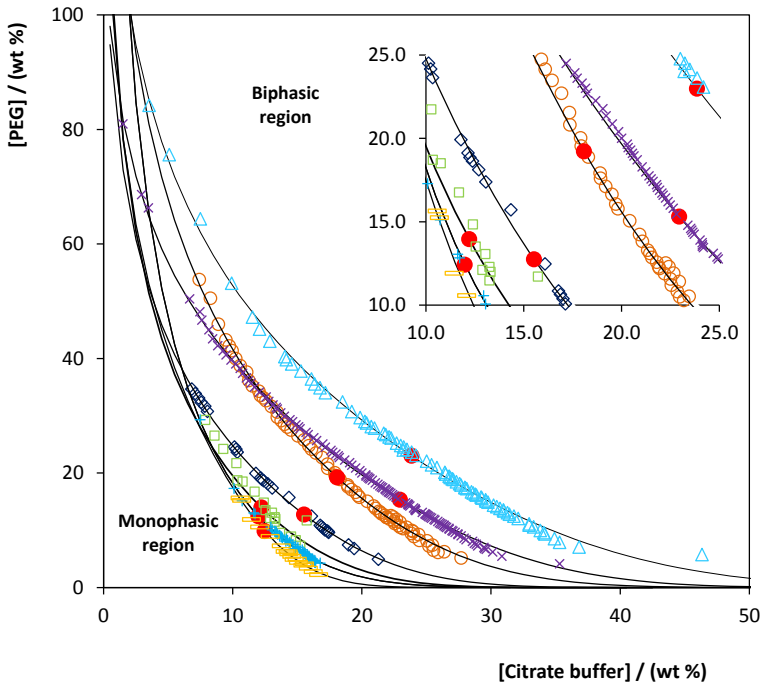

Figure 13: Evaluation of the molecular weight of PEG in the ternary phase diagrams composed of PEG + $C_6H_5K_3O_7$/$C_6H_8O_7$ + H_2O: PEG 400 (△); PEG 600 (×); PEG 1000 (○); PEG 2000 (◇); PEG 4000 (□); PEG 6000 (+) PEG 8000 (▫), and critical points of each system (●).

For the studied systems, the experimental binodal data were further fitted by the empirical relationship described by Equation (1). The regression parameters A, B and C, were estimated by the least-squares regression method, and their values and corresponding standard deviations (σ) are provided in Table 6. In general, good correlation coefficients were obtained for all systems, as it is possible to confirm in Figure 13, indicating that these fittings can be used to predict data in a given region of the phase diagram where no experimental results are available.

Table 6: Correlation parameters used to describe the experimental binodal data by Equation (1).

PEG	$A \pm \sigma$	$B \pm \sigma$	$10^5 (C \pm \sigma)$	R^2
400	167.4 ± 2.7	-0.360 ± 0.005	1.67 ± 0.67	0.9971
600	126.0 ± 0.9	-0.355 ± 0.003	3.36 ± 0.06	0.9986
1000	198.9 ± 7.3	-0.479 ± 0.012	5.06 ± 0.21	0.9981
2000	135.6 ± 6.0	-0.507 ± 0.016	9.83 ± 0.54	0.9991
4000	172.0 ± 17.7	-0.642 ± 0.039	14.6 ± 1.68	0.9983
6000	337.1 ± 38.2	-0.872 ± 0.041	16.3 ± 1.44	0.9953
8000	160.2 ± 138.4	-0.583 ± 0.292	37.6 ± 8.16	0.9947

The experimental TLs, along with their respective length (TLL), are reported in Table 7 as well as the composition of each system and respective pH values. An example of the TLs obtained is depicted in Figure 14; in general, the TLs are closely parallel to each other. In addition, the critical point of each system was also determined using equation (7) based on a geometrical approach schematized in Figure 14 for the system composed of PEG 400 + $C_6H_5K_3O_7/C_6H_8O_7$ + H_2O at pH 7. Their respective detailed data are presented in Appendix C, Table C. 1. In general, the contents of salt and PEG at the critical point are similar amongst the different systems, although the amount of each compound decreases with the increase of the PEG hydrophobicity – a consequence of their higher ability to create ABS.

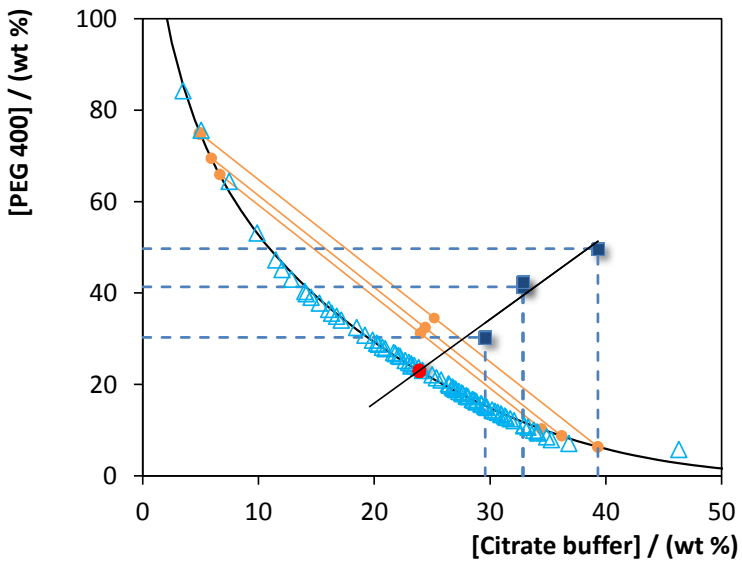

Figure 14: Phase diagram for the ternary system composed of PEG 400 + $C_6H_5K_3O_7/C_6H_8O_7$ + H_2O at pH 7, at 25 °C: binodal curve data (△,); TL data (●); adjusted binodal data through Equation 1 (-), critical point (●) and TL relation (■).

Table 7: Experimental data of TLs and TLLs of ABS composed of PEG + $C_6H_5K_3O_7$/$C_6H_8O_7$.

PEG	N.º	Weight fraction composition / wt %								TLL	α
		$[PEG]_{PEG}$	$[BUFFER]_{PEG}$	pH_{PEG}	$[PEG]_{M}$	$[BUFFER]_{M}$	$[PEG]_{BUFFER}$	[BUFFER] BUFFER	pH_{BUFFER}		
400	1	74.83	4.97	7.10	34.54	25.18	6.35	39.31	6.64	76.60	0.41
	2	42.43	13.64	6.82	24.86	24.64	11.78	32.83	6.80	36.17	0.57
	3	69.47	5.94	6.54	32.40	24.40	8.71	36.20	7.09	67.88	0.61
	4	65.91	6.66	6.49	31.17	24.00	10.24	34.45	6.98	62.22	0.62
	5	41.33	14.09	6.92	34.72	18.29	11.73	32.88	6.37	35.06	0.78
600	1	39.94	9.88	6.93	33.04	15.00	2.29	37.86	6.29	46.91	0.82
	2	34.81	11.96	6.71	18.86	23.32	4.56	33.50	6.58	37.14	0.47
	3	39.94	9.88	6.93	33.04	15.00	2.29	37.86	6.29	46.91	0.82
1000	1	55.62	6.90	6.22	26.18	24.61	0.90	40.15	6.30	64.49	0.47
	2	50.90	7.81	5.99	31.31	19.52	0.68	37.81	6.22	58.50	0.61
	3	36.65	11.39	6.17	19.39	20.72	4.61	28.71	6.19	36.41	0.46
2000	1	36.88	16.06	6.82	24.86	24.64	8.73	36.15	6.80	34.59	0.57
	2	51.33	10.46	6.54	32.40	24.40	2.80	46.20	7.09	60.30	0.61
	3	47.87	11.62	6.49	31.17	24.00	3.47	44.54	6.98	55.26	0.62
	4	30.28	19.46	6.64	24.33	23.50	15.35	29.59	6.75	18.04	0.60
4000	1	51.49	3.49	6.83	24.90	19.99	0.01	35.44	6.51	60.59	0.52
	2	42.23	4.68	6.79	24.75	15.04	0.12	29.65	6.48	48.95	0.58
	3	31.33	6.68	6.63	17.52	14.18	1.34	22.98	6.50	34.13	0.54
6000	1	21.53	9.09	6.41	15.05	12.03	4.22	16.94	6.37	19.00	0.63
	2	24.97	8.29	6.45	15.07	12.81	2.94	18.35	6.37	24.22	0.55
	3	27.33	7.80	6.45	12.22	14.96	1.95	19.82	6.32	28.08	0.40
	4	31.21	7.09	6.51	17.42	13.86	1.02	21.92	6.30	33.64	0.54
8000	1	23.49	8.45	6.42	12.02	14.16	0.64	19.83	6.41	25.53	0.50
	2	21.31	8.98	6.31	6.04	16.03	1.40	18.18	6.30	21.94	0.23
	3	30.03	7.02	6.53	16.46	14.10	0.13	22.61	6.37	33.72	0.55
	4	30.70	6.89	6.51	15.54	14.77	0.12	22.78	6.34	34.47	0.50

3.1.2. Effect of pH on the formation of PEG-salt based ABS

Aiming at studding the effect of pH on the ABS formation capacity, the respective liquid-liquid ternary phase diagrams for the system composed of PEG 400 + $C_6H_5K_3O_7$/$C_6H_8O_7$ + H_2O were determined at different pH values (5-9), using different ratios of potassium citrate and citric acid ($C_6H_5K_3O_7$/$C_6H_8O_7$). The phase diagrams obtained are depicted in Figure 15 (the experimental weight fraction data of each phase diagram are depicted in Appendix B, Table B. 5 and B. 6). The respective phase diagrams in molality units are presented in Appendix C, in Figure C. 3. It can be seen that the binodal curves have similar shapes for the different pH values, and that an increase in the pH leads to a higher ability for liquid-liquid demixing, being in agreement with literature for systems composed of polymers and other salts *(108)*. Note that, in general, the ability for ABS formation as a function of pH is strongly related with the speciation behaviour of citric acid or potassium citrate. Table 8 presents the pK_a values of citric acid. At pH values below 3.05 the non-charged citric acid is mainly present. At pH values above 4.67 and 5.39 there is the prevalence of the divalent and trivalent charged hydrogenocitrate and citrate anions, respectively (a weaker salting-out species if compared with the trivalent citrate anion). The same tendency was already observed for IL-salt based ABS *(109)*. It should be remarked that the phase diagram at pH 9 has already been reported by Lu *et al. (110)*, and the results obtained here display a good agreement with the literature (Appendix C, Figure C. 2).

Table 8: pK_a values of citric acid at 25 ^{o}C *(111)*.

pK_{a1}	pK_{a2}	pK_{a3}	pK_{a4}
3.05	4.67	5.39	13.92

The experimental binodal data were further fitted by the empirical relationship described by equation (1), with the respective representation shown in Figure 15, and the fitting parameters, standard deviations (σ) and correlation coefficients (R^2) are provided in Table 9. The experimental binodal data obtained lead to improved correlation coefficients indicating that these fittings can be used to predict data in a given region of the phase diagram where no experimental results are available.

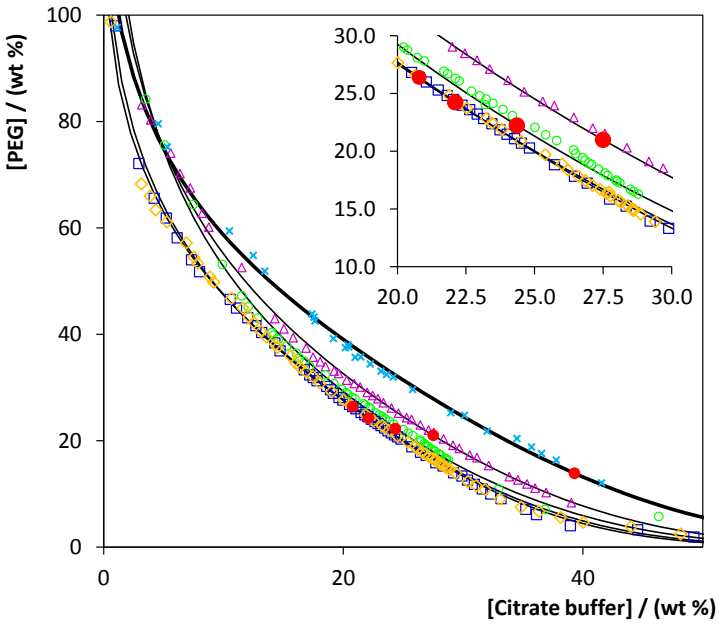

Figure 15: Ternary phase diagrams for systems composed of PEG 400 + $C_6H_5K_3O_7$/$C_6H_8O_7$ + H_2O at 25 °C and atmospheric pressure at different pH values: pH 5 (×), pH 6 (△), pH 7 (○), pH 8 (□) and pH 9 (◇), critical point (●).

The TLs, along with their respective length (TLL), are reported in Table 9. In addition, the critical point of each system is also depicted in Figure 15 with the detailed data shown in Appendix C, Table C. 2. In general, the compositions of the critical point become richer in PEG and poorer in salt with the increase of the pH.

Table 9: Correlation parameters used to describe the experimental binodal data by Equation 1.

PEG	pH	$A \pm \sigma$	$B \pm \sigma$	$10^5 (C \pm \sigma)$	R^2
	5	131.9 ± 2.1	-0.253 ± 0.006	1.10 ± 0.09	0.9979
	6	153.8 ± 3.0	-0.320 ± 0.007	1.51 ± 0.10	0.9967
400	7	167.4 ± 2.7	-0.360 ± 0.005	1.67 ± 0.67	0.9971
	8	127.2 ± 1.6	-0.305 ± 0.005	2.07 ± 0.10	0.9971
	9	119.4 ± 1.2	-0.285 ± 0.004	2.34 ± 0.08	0.9979

Table 10: Experimental data for TLs and TLLs of IL + $C_6H_5K_3O_7/C_6H_8O_7$ ABS, initial mixture compositions ($[PEG]_M$ and $[salt]_M$), and pH values of the coexisting phases.

PEG	pH	N.º	Weight fraction composition / wt %								TLL	α
			$[PEG]_{PEG}$	$[BUFFER]_{PEG}$	pH_{PEG}	$[PEG]_M$	$[BUFFER]_M$	$[PEG]_{BUFFER}$	$[BUFFER]_{BUFFER}$	pH_{BUFFER}		
400	5	1	63.58	8.20	5.66	28.64	35.35	3.19	55.13	5.51	76.48	0.58
		2	36.67	21.48	5.41	20.50	35.53	7.60	46.74	5.38	38.51	0.44
		3	32.90	23.97	5.43	19.88	35.40	8.71	45.21	5.36	32.19	0.46
	6	1	44.88	13.87	6.27	30.26	24.96	5.03	44.09	6.02	50.01	0.63
		2	50.57	11.59	6.27	32.24	26.13	2.53	49.69	6.11	61.32	0.62
		3	37.87	17.16	5.93	21.92	29.37	7.31	40.57	5.93	38.49	0.48
		4	74.83	4.97	7.10	34.54	25.18	6.35	39.31	6.64	76.60	0.41
		5	42.43	13.64	6.82	24.86	24.64	11.78	32.83	6.80	36.17	0.57
	8	1	47.16	10.13	7.76	26.99	25.38	3.12	43.44	7.70	55.22	0.54
		2	49.13	9.38	7.77	29.91	24.52	2.15	45.97	7.78	59.55	0.59
		3	40.01	13.21	7.64	24.24	24.46	7.38	36.49	7.63	40.09	0.52
		4	36.67	10.13	7.76	21.42	25.68	9.19	34.36	7.61	33.69	0.45
	9	1	48.19	9.68	7.86	27.01	25.02	3.30	55.55	8.04	55.55	0.53
		2	49.93	9.01	7.91	30.01	24.03	2.06	59.96	8.11	59.96	0.58
		3	40.69	2.97	7.84	24.25	24.25	8.11	35.01	7.90	39.33	0.50
		4	35.80	15.43	7.72	22.76	24.81	7.33	35.05	8.11	35.05	0.54

The pH values of the systems composed of PEG + $C_6H_5K_3O_7/C_6H_8O_7$ + H_2O are in the acid/neutral region (pH = 6 - 8) initially estimated and differences promoted by PEG practically were not observed in the buffered systems.

3.2. Extraction of IgG using PEG-salt based ABS

3.2.1. Extraction time

After the determination of all phase diagrams and respective TLs and TLLs, which allow to infer on the mixture compositions required to form two-phase systems, the following mixture compositions at pH ≈ 7 were applied to the extraction of IgG: 25 wt% of PEG 400 + 25 wt% of $C_6H_5K_3O_7/C_6H_8O_7$, 18 wt% of PEG 2000 + 16 wt% of $C_6H_5K_3O_7/C_6H_8O_7$, and 16 wt% of PEG 8000 + 15 wt % of $C_6H_5K_3O_7/C_6H_8O_7$ (which correspond to a TLL of *circa* 35). This study was carried out in order to understand the best time conditions for the extraction and purification of IgG (aiming at avoiding precipitation and denaturation effects while guarantying the equilibrium conditions). Pure IgG aqueous solutions were used at this stage. The first extractions were carried out with the ABS composed of the lower and highest molecular weight PEGs, namely 400 and 8000 $g \cdot mol^{-1}$. It is important to refer that in the systems composed of PEG 400 the protein precipitation was not

observed, while all samples composed of PEG 8000, exposed at different times of extraction demonstrated as the presence of some precipitated proteins, as shown in Figure 16. Thus, based on these visual inspections, the results shown in Figure 17, with the respective data in Appendix D, Table D.1, confirm the higher yield of IgG (Y_{IgG}) obtained with the systems composed of PEG 400. In particular, the best results were obtained with the phases' separation promoted by centrifugation at 1000 rpm for 10 min followed by 120 min of rest, and for the 300 and 720 min without the use of centrifugation.

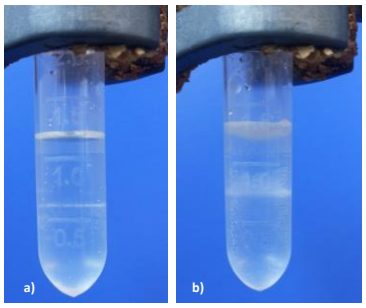

Figure 16: Extraction of IgG using ABS constituted by PEG + $C_6H_5K_3O_7$/$C_6H_8O_7$ at 25 ^{o}C, a) PEG 400 and b) PEG 8000.

Although with the systems formed by PEG 400 it was not visually detected the protein precipitation, yields lower than 50 % were obtained in all studies – Figure 17. The low amounts of protein loss are not macroscopically seen. In all situations, PEG 400 leads to higher extraction efficiencies when compared with the results afforded by PEG 8000. IgG preferentially migrates for the polymer-rich phase in systems composed of PEG 400 (EE_{IgG} % ranging between 88 and 96 %), while the results obtained for PEG 8000 show a more distinct behavior and preferential extraction to the polymer- or salt-rich phases depending on the conditions applied to promote the phase separation (EE_{IgG} % ranging between 23 and 66 %). These more pronounced differences can be a direct result of the higher viscosity of aqueous solutions of PEG 8000. Moreover, and for the results in which centrifugation was applied, PEG 400 leads to lower losses of protein.

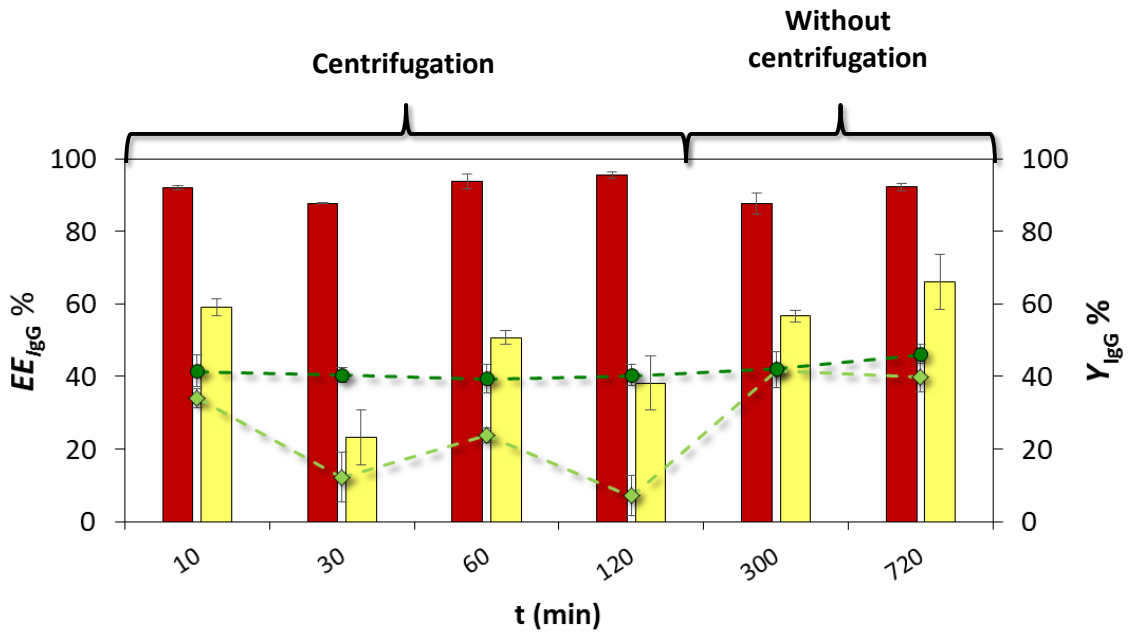

Figure 17: Extraction efficiencies (EE_{IgG} %) and extraction yields (Y_{IgG} %) of IgG using ABS composed of PEG 400 and PEG 8000 at pH≈7 and at 25 °C: EE_{IgG} % PEG 400 (■) and Y_{IgG} % (——); EE_{IgG} % PEG 8000 (■) and Y_{IgG} % (——). Extraction times of 10 to 120 min, before 10 min of centrifugation at 1000 rpm and 300 and 720 min without centrifugation.

Andrews *et al*. *(68)* demonstrated that hydrophobic proteins partition preferentially to the PEG-rich phase in polymer-salt ABS *(68)*. Thus, it is expected that IgG has a higher preference for the polymer-rich phase when more hydrophilic polymers (of lower molecular weight) are used considering its large its low surface hydrophobicity, 14% *(6,44)*. Moreover, due to the high IgG molecular weight (150 kDa) size-exclusion effects are also observed in systems constituted by polymers of higher molecular weight. These trends can be observed in more detail by the analysis of the partition coefficients represented in Figure 18. In all situations, the partition coefficients (Appendix D, Table D. 1) obtained with the systems formed by PEG 400 are higher than those observed with the ABS formed by PEG 8000.

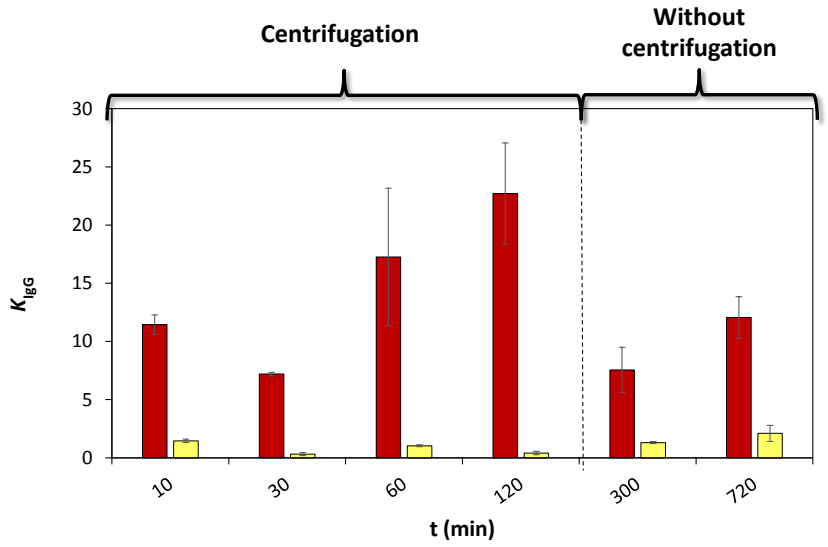

Figure 18: Partition coefficient of rabbit IgG (K_{IgG}) in different ABS, composed of PEG 400 and PEG 8000 at pH≈7 and at 25 °C: PEG 400 (■) and PEG 8000 (■).Extraction times of 10 to 120 min, before 10 min of centrifugation at 1000 rpm and 300 and 720 min without centrifugation.

As the PEG alkyl chain length decreases, there will be less ethylene oxide groups *per* PEG molecule, for the same concentration of polymer, and hence the top phase will be less hydrophobic. On the other hand, a decrease in the PEG molecular weight leads to a decrease in the steric exclusion of proteins from the PEG-rich phase *(6)*. In fact, our results suggest that lower molecular weight PEGs are favourable for the partitioning of IgG, and as previously suggested by Yan-Min *et al. (107)* who reported the extraction and back-extraction of bovine serum albumin (BSA) with PEG/potassium citrate ABS, as well as in the studies of Aires Barros *et al*. *(3)* regarding the IgG partition in PEG/ phosphate (with 15% of NaCl).

After the analysis of the previous results, the best conditions for the systems composed of PEG 400 and 8000 were chosen and another time of equilibrium, 180 min, was included to complete this study. However, short times of extraction were chosen to avoid the contact of the protein for long periods when the IL is included as well as aiming at developing a scalable technique. The subsequent studies were performed submitting the systems at different times of rest namely, 60, 120 and 180 min. Before, the same systems were submitted to 10 min of centrifugation, at 1000 rpm. This procedure was applied also to the ABS composed of PEG 2000.

The results obtained in terms of extraction efficiencies are depicted in Figure 19. Higher *EE*% values were obtained for PEG 400. Moreover, as expected by the previous results, the best yields were obtained for PEG 400, then for PEG 2000 and finally for PEG 8000 (the respective values are

presented in Appendix D, Table D. 2). However, in average, there is a loss of IgG of about 60%. The only exception was for PEG 2000 with 180 min of rest, where it was observed a loss of the protein around 35%. This result is however not very consistent, because in this ABS it was possible to see a significant amount of precipitated proteins, such as in the same type of ABS for the others two times of extraction. Taking into account that all samples composed of PEG 2000 and 8000 shown turbidity (protein precipitation in the systems interface), the values determined (EE_{IgG} %, K_{IgG} and Y_{IgG} %) may not be completely accurate.

As expected by the previous results, IgG preferentially migrates for the PEG-rich phase (TP) in the cases where the polymer has a lower molecular weight, and as shown in the partition coefficients trend shown in Figure 20.

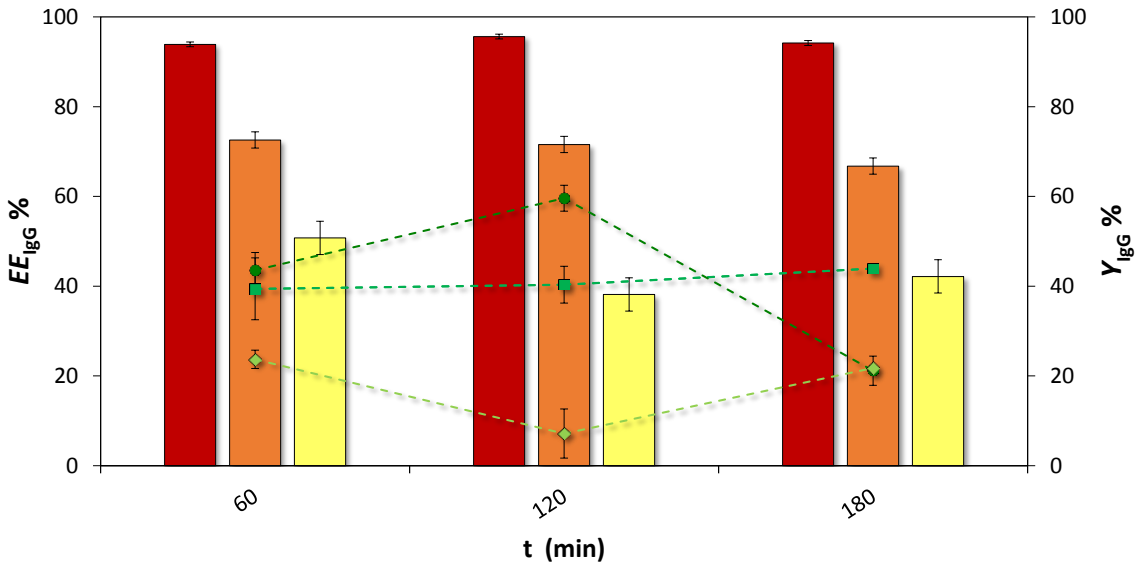

Figure 19: Percentage extraction efficiencies (EE_{IgG} %) and extraction yield (Y_{IgG} %) of IgG using different ABS composed of PEG 400, 2000 and PEG 8000 at pH≈7 and at 25 °C: EE_{IgG} % PEG 400 (■) and Y_{IgG} % (——); EE_{IgG} % PEG 2000 (■); and Y_{IgG} % (——); EE_{IgG} % PEG 8000 (■) and Y_{IgG} % (——).

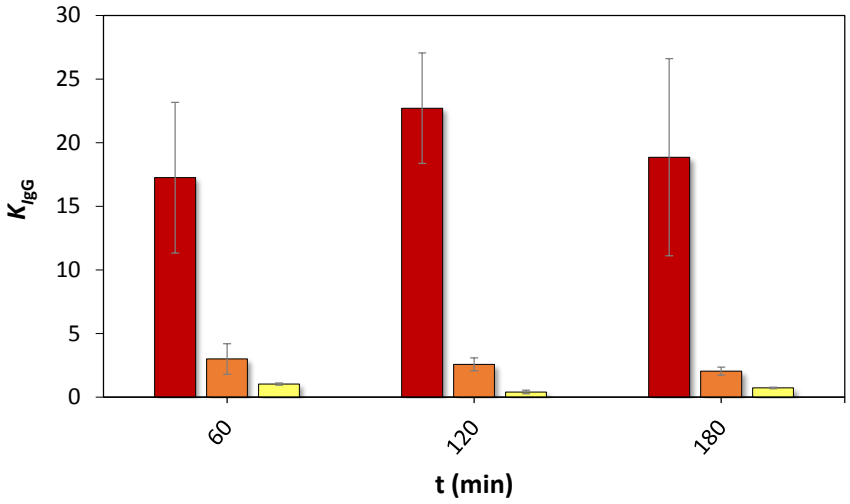

Figure 20: Partition coefficient of rabbit IgG (K_{IgG}) in different ABS, composed of PEG 400, 200 and 8000 at pH≈7 and at 25 ^{o}C: K_{IgG} PEG 400 (■);K_{IgG} PEG 2000 (■);K_{IgG} PEG 8000 (■).

The best results, taking into account the IgG extraction efficiency and yield, were achieved with 120 min of rest time before the 10 min of centrifugation at 1000 rpm. Thus, this procedure was applied to the remaining and subsequent experiments.

3.2.2. Effect of the polymer molecular weight

In this section, the extraction and yield of IgG using ABS composed of PEGs of different molecular weight + $C_6H_5K_3O_7/C_6H_8O_7$ + H_2O (pH ≈ 7) were investigated. For the interpretation of results, it is necessary to take into account the findings of P. A. Albertsson *(112)*, who described a model for the partition of proteins, where the partition coefficient (*K*) can be affected by different factors, such as salt type and concentration, pH and temperature, as well as the electrochemical, hydrophobic and size of the proteins. Later, a linear relation was proposed by Asenjo *et al. (113)* to relate the partition coefficient and the hydrophobicity of proteins in ABS. In summary, the partition of proteins in ABS are dependent on hydrophobic-type interactions, electrostatic forces, molecular size, solubility, and affinity for both phases, and their magnitudes further depend on the two-phase compositions and on the nature of the phase-forming components *(9)*.

Furthermore, in the systems studied of the type polymer-salt, the *K* of proteins is mainly governed by volume exclusion (polymer-rich phase) and salting-out effects (salt-rich phase) *(62)*. However, electrostatic interactions cannot be discarded if extractions are being carried out at pH values different from the protein pI as well as hydrogen-bonding interactions, which seem particularly relevant in water-rich media. According to the literature, PEGs of higher molecular

weight lead to lower extraction efficiencies for the polymer-rich phase due to volume-exclusion effects *(3,114)*. According to our results, shown in Figures 21 and 22, a similar trend was observed. Nevertheless, the overall size-exclusion *(115,116)* and salting-out effects *(115,116)*, as well as specific interactions *(117)*, cannot be discarded through the IgG partitioning.

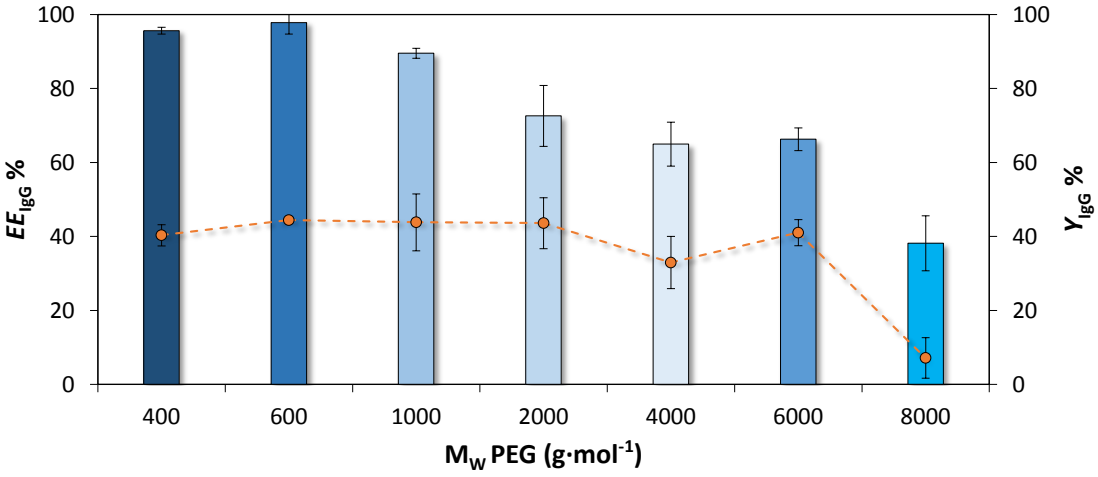

Figure 21: Percentage extraction efficiencies (EE_{IgG} %) and yield (Y_{IgG}%) of rabbit IgG in different ABS formed by PEG 400 to PEG 8000 at pH≈7 and at 25 °C: EE_{IgG} % for PEG 400 (■), PEG 600 (■), PEG 1000 (■), PEG 2000 (■), PEG 4000 (■), PEG 6000 (■), PEG 8000 (■). The line corresponds to the recovery yields of IgG in the same systems Y_{IgG} % (——).

The best results, in terms of EE_{IgG} % and Y_{IgG} %, were achieved with the systems formed by PEG 400 and PEG 600 (Appendix D, Table D. 3). These results demonstrate that polyclonal antibodies have a higher tendency to migrate to the PEG-rich phase for lower molecular weight PEGs. For the remaining tested PEGs (1000, 2000, 4000, 6000 and 8000 g·mol^{-1}), the EE_{IgG} % and *K* values were lower than those observed for the systems formed by PEG 400 or 600, in addition that protein precipitation and turbidity was macroscopically visible with PEG 2000, 4000, 6000 and 8000. This evidence was previously described by Rosa *et al. (6)*, in which the protein precipitation was observed for higher PEG molecular weights, leading to lower yields.

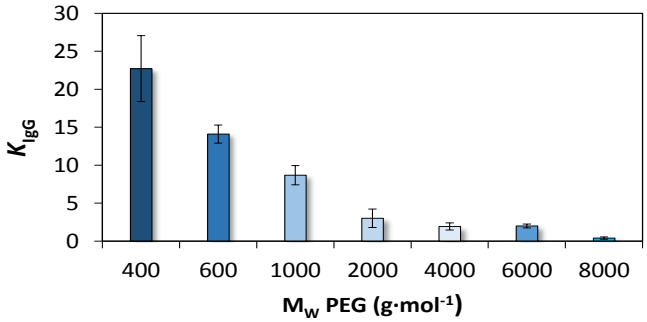

Figure 22: Partition coefficient (K_{IgG}) of rabbit IgG in different ABS composed of PEG 400 to PEG 8000 at pH≈7 and at 25 °C: PEG 400 (■), PEG 600 (■), PEG 1000 (■), PEG 2000 (■), PEG 4000 (■), PEG 6000 (■), PEG 8000 (■).

Taking into account the results obtained for EE_{IgG} %, Y_{IgG} % and K_{IgG}, and the best results achieved with the low molecular weight polymers, the following experiments were carried out with ABS formed by PEG 400.

3.2.3. Effect of pH

The pI of rabbit IgG is 7.8, meaning that at this pH the protein has a nearly zero net charge and thus no electrostatic interaction occur *(116)* while protein-polymer interactions seem to determine the partition behavior *(118,119)*. It was already demonstrated that the pH in PEG/salt systems affect the partition of IgG *(114,120)*. In fact, several researchers reported that at higher pH values the negatively charged biomolecule prefers the top phase (polymer-rich) *(120)*. The extraction efficiencies and recovery yield of IgG in ABS composed of PEG 400 + $C_6H_5K_3O_7$/$C_6H_8O_7$ + H_2O at different pH values and at 25 °C are shown in Figure 23 (detailed data in Appendix D, Table D. 4). In all systems, EE_{IgG}% higher than 95% and Y_{IgG}% ranging between 46 and 49 % were obtained. Although no major differences are observed in the extraction efficiencies, the partition coefficients shown in Figure 24, confirm the affinity of IgG for the polymer-rich phase, which is increased at the pH values of 8 and 9.

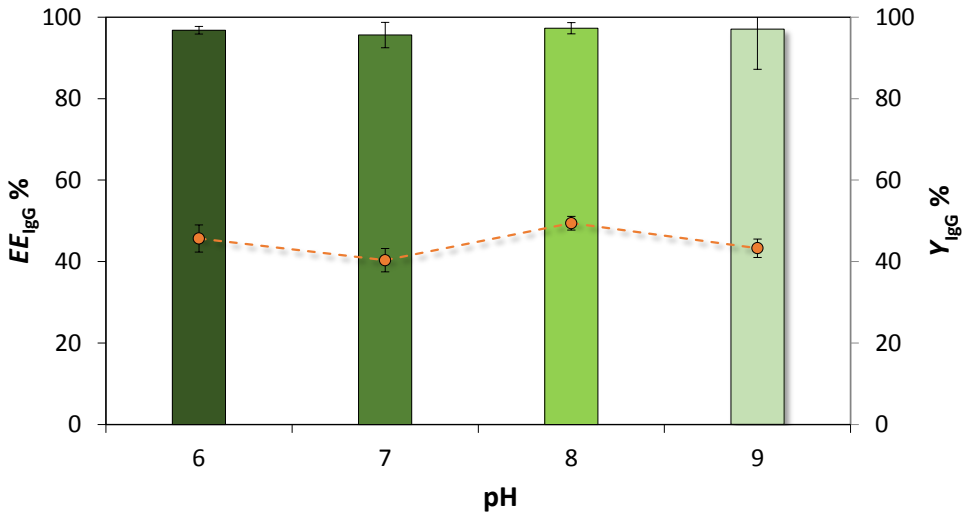

Figure 23: Percentage extraction efficiencies of rabbit IgG (EE_{IgG}*%)* in the ABS composed of PEG 400 + $C_6H_5K_3O_7/C_6H_8O_7$ + H_2O at different pH values and at 25 ºC. The line corresponds to the recovery yields of IgG in the same systems Y_{IgG} % (——).

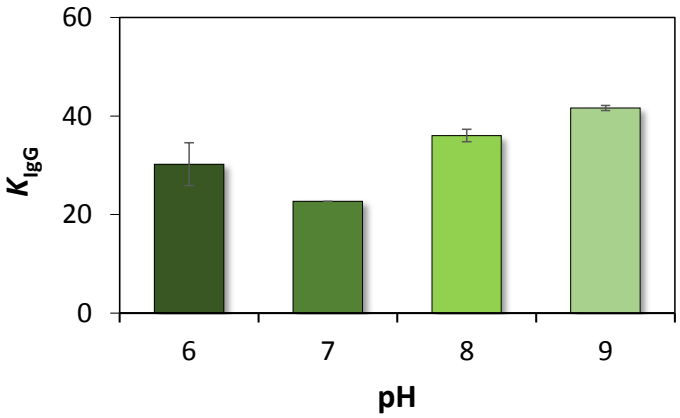

Figure 24: Effect of pH on the partition coefficient of rabbit IgG (K_{IgG}) in the ABS composed of PEG 400 + $C_6H_5K_3O_7/C_6H_8O_7$ + H_2O at different pH values and at 25 ºC.

When the pH is increased, the protein becomes more negatively charged. Aires Barros *et al. (2)* evaluated the extraction and precipitation of human IgG at different pH values, ranging from 3 to 8, with PEG 3350/Dextran systems. The authors *(2)* observed a severe precipitation (over 50%) in the pH range 5–8; but at more acidic values precipitation was considerable reduced. In our study, the precipitation of the protein was not macroscopically visible although our yields of IgG are always below 50% and with no major differences amongst the several pH values investigated (Figure 23). Therefore, further studies at lower pH values must be conducted in the near future

trying at overcoming this large loss of IgG with the systems investigated. Hatta *et al.(36)* studied the IgG stability and specific activity as a function of temperature and pH by differential scanning calorimetry (DSC) and ELISA. It was demonstrated that IgG is stable at 60 °C – 70 °C for 10 min while an activity loss of IgG of 10% occurs at pH values from 4-9 at 37 ^{o}C *(36)*. Since no major differences were observed at the pH values investigated, the remaining studies were carried out at the initial pH value, pH ≈7.

3.3. Extraction of IgG using ILs as adjuvants in PEG-salt based ABS

3.3.1. Effect of the IL anion

The capacity to extract and partition IgG into PEG 400 + $C_6H_5K_3O_7$/$C_6H_8O_7$ + H_2O (pH≈7) ABS, in the presence of various ILs, was investigated herein. This study started taking account the effect of the IL anion nature through the IgG extraction and recovery, by keeping the IL with a common imidazolium cation ($[C_4mim]^+$) combined with the following anions: Cl^-, $[TOS]^-$, Br^-, $[CH_3CO_2]^-$ and $[N(CN)_2]^-$. A common mixture composition was chosen 25 wt% of PEG 400 + 25 wt% of $C_6H_5K_3O_7$/$C_6H_8O_7$ + 5% IL , pH ≈ 7 at 25 ^{o}C with the addition of several ILs at 5 wt% to the overall mixture. Figure 25 depicts the extraction efficiency of IgG in the several systems investigated (the respective values are presented in Appendix D, Table D. 5). According to the obtained results, the EE_{IgG}% follows the IL anions trend: $[TOS]^- \approx [CH_3CO_2]^- \approx Cl^- > [N(CN)_2]^- > Br^-$. In summary. an increase in the EE_{IgG}% from 96 % (with no IL added) to 100% or complete extraction in a single-step was observed with the systems composed of 5 wt% of the following ILs: $[C_4mim][TOS]$, $[C_4mim][CH_3CO_2]$ and $[C_4mim]Cl$. On the other hand, the systems with $[C_4mim]Br$ lead to EE_{IgG}% 89%, respectively, *i.e.*, a decrease on the EE_{IgG}% when compared with the ABS where no IL was added (Figure 25). However, this IL leads to a slight increase on the recovery yield of IgG. The hydrogen-bond basicity is a measure of the ability of a compound to accept a proton (or donate an electron pair) in a solute-solvent hydrogen-bond *(121)*. In fact, the values of the IL anions hydrogen-bond basicity follows the rank: $[CH_3CO_2]^- > Cl^- > Br^- > [N(CN)_2]^-$ *(121)*, meaning that a decrease on the IL anion hydrogen-bond basicity leads to a decrease on the extractions efficiencies. These results are also in accordance with the Hofmeister series where stronger salting-out anions induce the protein precipitation *(122)*.

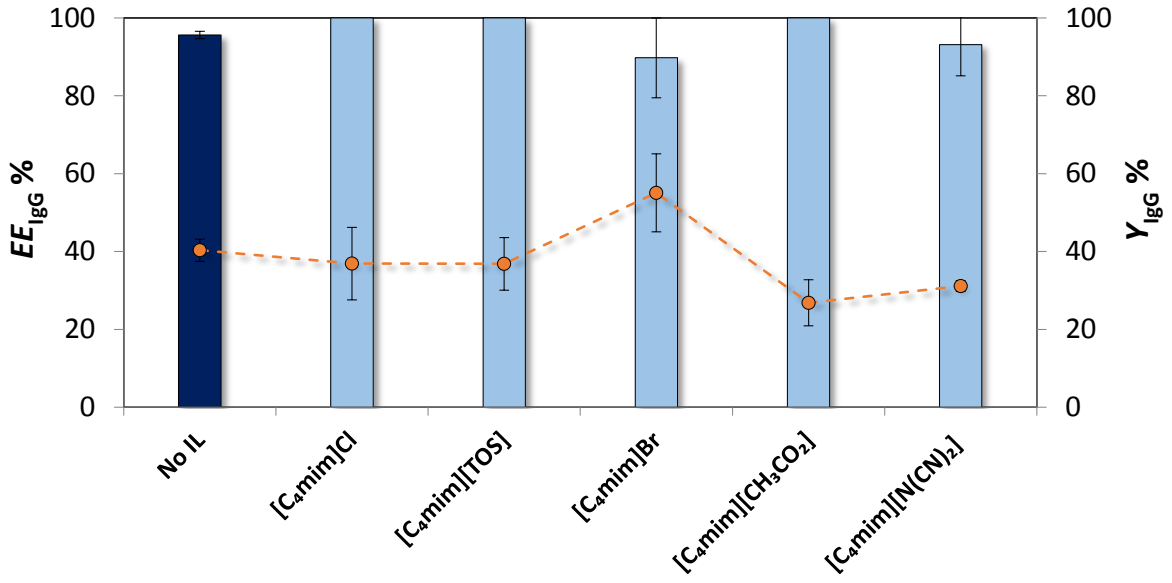

Figure 25: Percentage extraction efficiencies of rabbit IgG, EE_{IgG}%, using ABS composed of PEG 400 + $C_6H_5K_3O_7/C_6H_8O_7$ + H_2O and [C_4mim]-based ILs at 5 wt%, at pH≈7 and 25 °C. The first bar corresponds to the ABS where no IL was added. The line corresponds to the recovery yields of IgG in the same systems Y_{IgG} % (——).

Kosmotropic cations (strongly hydrated) are considered as 'structure-makers' because they increase the protein stability in solution. On the other hand, chaotropic ions (weakly hydrated) are the 'structure breakers' and decrease the stability of proteins in aqueous medium *(122)*. The Hofmeister series is shown in Figure 26 *(123)*.

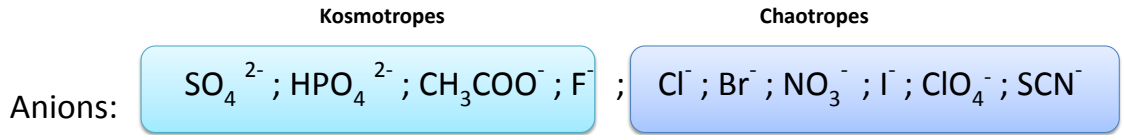

Figure 26: The Hofmeister series and the ions ranking (adapted from *(124)*).

3.3.1. Effect of the IL cation

The effect of the IL cation alkyl side chain length was finally ascertained, using 5 wt% [$C_n$mim]Cl (n = 2, 4, 6, 8, 10, 12 and 14) in the ABS formed by 25 wt% of PEG 400 + 25 wt% of $C_6H_5K_3O_7/C_6H_8O_7$ + 5% IL , pH ≈ 7 at 25 °C. For the common mixture composition used the results show that EE_{IgG}% decreases in the order: [C_2mim]Cl ≈ [C_4mim]Cl ≈ [C_6mim]Cl ≈ [C_{12}mim]Cl > [C_{14}mim]Cl > [C_{10}mim]Cl > [C_8mim]Cl (Figure 27, with the respective values presented in Appendix

D, Table D. 6). With [C_2mim]Cl, [C_4mim]Cl, [C_6mim]Cl and [C_{12}mim]Cl the EE_{IgG}% obtained reached 100%, i.e., a complete extraction of IgG for the polymer-rich phase in a single step. However, the Y_{IgG}% in these systems ranges between 22 and 36 %. Remarkably, the ABS composed of [C_{10}mim]Cl led to a significant increase in the IgG stability and recovery, and from 40 % (where no IL was added) to 81 % (Figure 27). A possible explanation, is the fact that an increase of the cation/anion alkyl side chain length leads to an increase on the IL hydrophobicity (9), and it was already reported that proteins are more stable in hydrophobic ILs *(125)*. Others studies in the literature demonstrated that [C_8mim]- and [C_{10}mim]-based ILs are good candidates for the extraction of proteins. Ventura *et al. (126)* demonstrated the activity increase of an enzyme promoted by the self-aggregation of [C_{10}mim]Cl. The self-aggregation of the IL is responsible for the increase in the IL–water interface, and consequently, for the increase in the enzyme activity and stability. Souza *et al. (82)* additionally demonstrated that the use of [C_8mim]Cl as an adjuvant promotes the preferential partition of the proteins for the top phase of a conventional ABS (PEG-rich phase).

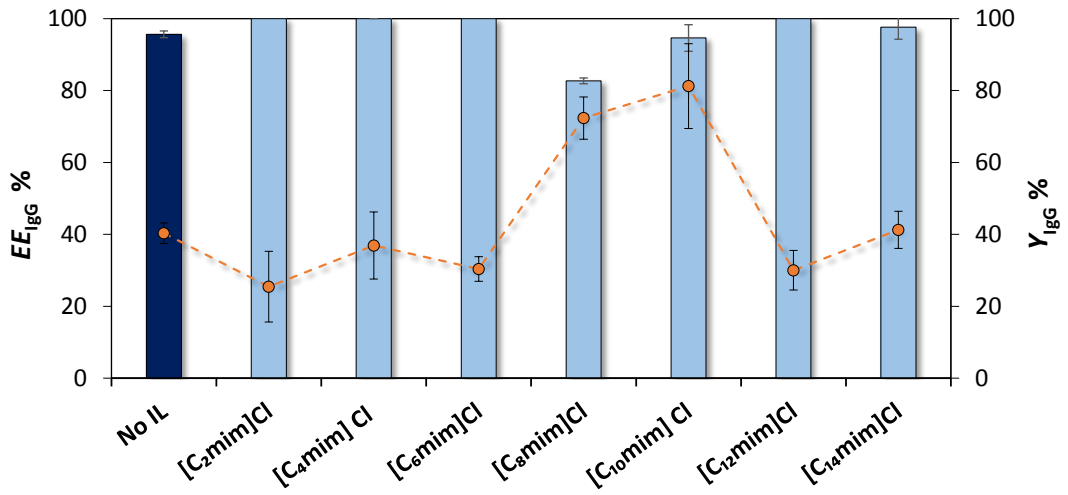

Figure 27: Percentage extraction efficiencies of rabbit IgG, EE_{IgG}% ,for different chain length of [$C_n$mim]Cl (n = 2, 4, 6, 8, 10, 12, 14): ABS composed of PEG 400 + $C_6H_5K_3O_7$/$C_6H_8O_7$ + H_2O and [$C_n$mim]Cl at 5 wt%, at pH≈7 and 25 °C. The first bar corresponds to the ABS where no IL was added. The line corresponds to the recovery yields of IgG in the same systems Y_{IgG} % (——).

Comparing the results obtained with the ABS composed of 5 wt% of different ILs shown in**Error! Reference source not found.**Figure 27, added as adjuvants to PEG 400 + $C_6H_5K_3O_7$/$C_6H_8O_7$ + H_2O at pH ≈ 7 ABS, it can be concluded that most of the ILs lead to an increase in the EE_{IgG}%. To

other ABS with 5% IL, EE_{IgG} % was possible to obtain 100 %. In terms of Y_{IgG} % was shown it is also possible to improve. Moreover, Ranyere L. S. *et al.*, study the use of imidazolium-based ILs as adjuvants (5 wt%) in ABS of polyethylene glycol systems (1500, 4000, 6000 and 8000 g mol^{-1}) with potassium phosphate buffer at pH 7, in the extraction and purification of a lipase, and obtained a high purification factor *(82)*.

In summary, the use of ILs as adjuvants allows to tailor either the extraction efficiency or the recovery yield of IgG. Form the obtained results, the correct choice of the anion and cation that composes a given IL can allow the increase of both the extraction efficiency and yield. However, further studies are still required at this stage, namely on the study of the concentration of the $[C_{10}mim]Cl$ in order to check if higher extraction efficiencies and recoveries of IgG can be even attained.

4. Final remarks

4.1. Conclusions

The main purpose of this work consisted on the development of an alternative and efficient approach for the extraction and purification of immunoglobulin G. To this end, the binodal curves of ABS composed of different PEGs (400, 600, 1000, 2000, 4000, 6000 and 8000) and ($K_3C_6H_5O_7$/$C_6H_8O_7$) at pH ≈7 at 25 ^oC were determined. The ABS formation ability follows the trend: PEG 8000 > PEG 6000 > PEG 4000 > PEG 2000 > PEG 1000 > PEG 600 > PEG 400, meaning that higher molecular weight polymers are more able to form ABS in the presence of a given salt. Further, the binodal curves for the ABS formed by PEG 400 and $K_3C_6H_5O_7$/$C_6H_8O_7$ at different pHs (5 to 9) were determined. The ability of $K_3C_6H_5O_7$/$C_6H_8O_7$ to induce the formation of PEG-based ABS decreases with an increase in the pH of the medium. In addition, several TLs and respective TLLs were also determined to characterize the investigated systems. In summary, these experiments were carried out to characterize the ABS under investigation, aiming at inferring on the mixture compositions required to form two-phase systems and to work at similar TLLs during the partition experiments.

Regarding the extraction experiments, initially, the operational conditions used for the two-phase separation were evaluated in terms of extraction efficiency and recovery yield of IgG. Afterwards, the molecular weight of PEG as phase-forming components of ABS was evaluated. Extraction efficiencies of 96 % and 98 % were obtained for the systems composed of PEG 400 and PEG 600, respectively. Moreover, in terms of Y_{IgG}%, the best results achieved were also with PEG 400 (40 %) and PEG 600 (44 %). The pH of the ABS were also tested; yet, in the pH range evaluated (6-9) no significant differences were observed in terms of EE_{IgG}% (95 to 97%) and recovery yields (40 to 49 %).

Finally, and aiming at both increasing the extraction efficiency and recovery yield of IgG, it was explored the use of ILs as adjuvants in ABS. Several ILs were tested in order to analyse the IL cation alkyl side chain length and anion influence. EE_{IgG}% of 100% were achieved with the ILs [C_4mim][TOS], [C_4mim][CH_3CO_2], [C_4mim]Cl, [C_2mim]Cl, [C_4mim]Cl, [C_6mim]Cl and [C_{12}mim]Cl. However, the obtained Y_{IgG} were lower than 40%. Otherwise, it was not possible to obtain values of 100% of EE_{IgG}% with [C_4mim]Br,[C_4mim][$N(CN)_2$], [C_8mim]Cl and [C_{10}mim]Cl. Nevertheless, remarkable results were achieved for Y_{IgG} (reaching a value of 81 % with the IL [C_{10}mim]Cl).

The results obtained reveal a high affinity of IgG for the polymer-rich phase; although, the complete extraction of IgG was never attained in a single-step in systems where no ILs are added. After the addition of 5 wt% of adequate ILs, extraction efficiencies of 100% of IgG were obtained, as well as, remarkable higher yields. From this work, it is clear that low amounts of ILs in the

formulation of ABS are enough to trigger complete extractions of target compounds in a single-step. Thus, ABS composed of PEG, biodegradable organic salts and ILs (as adjuvants), can be envisaged as an alternative and more efficient method for the purification of biopharmaceuticals.

4.2. Future work

More ILs can be tested, in order to obtain higher Y_{IgG}% and EE_{IgG}%, and then apply the improved systems to purify IgG from rabbit serum. After the purification of IgG, its recuperation from the PEG-rich phase should be addressed, as well as the recycling nature of the ABS used. Additional investigations regarding the effects of the phase-forming components through the protein stability and activity are also required.

5. References

(1) A., T. P., and Brogden, R. N. (1989) Muromonab CD3. A review of its pharmacology and therapeutic potential. *Drugs 37*, 871–899.

(2) Silva, M. F. F., Fernandes-Platzgummer, A., Aires-Barros, M. R., and Azevedo, A. M. (2014) Integrated purification of monoclonal antibodies directly from cell culture medium with aqueous two-phase systems. *Sep. Purif. Technol. 132*, 330–335.

(3) Azevedo, A. M., Rosa, P. A. J., Ferreira, I. F., and Aires-Barros, M. R. (2007) Optimisation of aqueous two-phase extraction of human antibodies. *J. Biotechnol. 132*, 209–217.

(4) Rosa, P. A. J., Azevedo, A. M., Sommerfeld, S., Mutter, M., Bäcker, W., and Aires-Barros, M. R. (2013) Continuous purification of antibodies from cell culture supernatant with aqueous two-phase systems: from concept to process. *Biotechnol. J. 8*, 352–362.

(5) Martínez-Aragón, M., Burghoff, S., Goetheer, E. L. V., and Haan, A. B. (2009) Guidelines for solvent selection for carrier mediated extraction of proteins. *Sep. Purif. Technol. 65*, 65–72.

(6) Rosa, P. A. J., Azevedo, A. M., and Aires-Barros, M. . R. (2007) Application of central composite design to the optimisation of aqueous two-phase extraction of human antibodies. *J. Chromatogr. A 1141*, 50–60.

(7) Ferreira, I. . F., Azevedo, A. M., Rosa, P. A. J., and Aires-Barros, M. R. (2008) Purification of human immunoglobulin G by thermoseparating aqueous two-phase systems. *J. Chromatogr. A 1195*, 94–100.

(8) Passos, H., Ferreira, A. R., Cláudio, A. F. M., Coutinho, J. A. P., and Freire, M. G. (2012) Characterization of aqueous biphasic systems composed of ionic liquids and a citrate-based biodegradable salt. *Biochem. Eng. J. 67*, 68–76.

(9) Pereira, J. F. B., Lima, Á. S., Freire, M. G., Coutinho, J. A., and P., . (2010) Ionic liquids as adjuvants for the tailored extraction of biomolecules in aqueous biphasic systems. *Green Chem. 12*, 1661–1669.

(10) Louros, C. L. S., Cláudio, A. F. M., Neves, C. M. S. . S., Freire, M. G., Marrucho, I. M., Pauly, J., and Coutinho, J. A. P. (2010) Extraction of biomolecules using phosphonium-based ionic liquids + K(3)PO(4) aqueous biphasic systems. *Int. J. Mol. Sci. 11*, 1777–1791.

(11) Elgert, K. D. (2009) Antibody structure and function, in *Immunology - Understanding the Immune System*, pp 58–78.

(12) Leenaars, M., and Hendriksen, C. F. M. (2005) Critical steps in the production of polyclonal and monoclonal antibodies: evaluation and recommendations. *ILAR J. 46*, 269–279.

(13) Malpiedi, L. P., A., D. C., Nerli, B. B., and Pessoa Jr., A. (2013) Single-chain antibody fragments: Purification methodologies. *Process Biochem. 48*, 1242–1251.

(14) Kindt, J. T., Golddsby, A. R., and Osborne, A. B. (2007) Kuby Immunology (Freeman, W. H., Ed.) 6th ed. New York.

(15) Thermo Scientific Pierce Antibody Production and Purification Technical Handbook 2 Version.

(16) Lipman, N. S., Jackson, L. R., Trudel, L. J., and Weis-Garcia, F. (2005) Monoclonal Versus Polyclonal Antibodies: Distinguishing Characteristics, Applications, and Information Resources. *ILAR J. 46*, 258–268.

(17) Köhler, G., and Milstein, C. (1975) Continuous cultures of fused cells secreting antibody of predefined specificity. *Nature 256*, 495–497.

(18) http://www.abcam.com/protocols/a-comparison-between-polyclonal-and-monoclonal.

(19) Nelson, P. N., Reynolds, G. M., Waldron, E. E., Ward, E., Giannopoulos, K., and Murray, P. G. (2000) Demystified...monoclonal antibodies. *J. Clin. Pathol. Pathol. 53*, 111–117.

(20) Rosa, P. A. J., Azevedo, A. M., Ferreira, I. F., Sommerfeld, S., Bäcker, W., and Aires-Barros, M. R. (2009) Downstream processing of antibodies: single-stage versus multi-stage aqueous two-phase extraction. *J. Chromatogr. A 1216*, 8741–8749.

(21) Azevedo, A. M., Gomes, A. G., Rosa, P. A. J., Ferreira, I. F., Pisco, A. M. M. O., and Aires-Barros, M. R. (2009) Partitioning of human antibodies in polyethylene glycol–sodium citrate aqueous two-phase systems. *Sep. Purif. Technol. 65*, 14–21.

(22) Wang, Y., Lomakin, A., Latypov, R. F., Laubach, J. P., Hideshima, T., Richardson, P. G., Munshi, N. C., Anderson, K. C., and Benedek, G. B. (2013) Phase transitions in human IgG solutions. *J. Chem. Phys. 139*, 121904–1–121904–9.

(23) Penha, T. R., Krüger, E. R., Thomaz-soccol, V., Victor, J., Agottani, B., Itano, F. H., Della, L., and Troiano, C. (2010) Production and Characterization of Monoclonal Antibodies Anti Fragment Fc of Bovine IgG. *Brazilian Arch. Biol. Technol. Technol. 53*, 105–114.

(24) Monkos, K., and Turczynski, B. (1999) A comparative study on viscosity of human, bovine and pig IgG immunoglobulins in aqueous solutions. *Int. J. Biol. Macromol. 26*, 155–159.

(25) Gagnon, P. (2012) Technology trends in antibody purification. *J. Chromatogr. A 1221*, 57–70.

(26) Ayyar, B. V., Arora, S., Murphy, C., and O'Kennedy, R. (2012) Affinity chromatography as a tool for antibody purification. *Methods 56*, 116–29.

(27) Gelfand, E. W. (2006) Differences between IGIV products: impact on clinical outcome. *Int. Imunopharmacology 6*, 592–599.

(28) Pinheiro, A., Woof, J. M., Almeida, T., Abrantes, J., Esteves, P. J., Alves, P. C., and Gortázar, C. (2014) Leporid immunoglobulin G shows evidence of strong selective pressure on the hinge and CH3 domains 1–9.

(29) Nikolayenko, I. V, Galkin, O. Y., Grabchenko, N. I., and Spivak, M. Y. (2005) Preparation of highly purified human IgG , IgM , and IgA for immunization and immunoanalysis. *Ukr. Biooganica Acta 2*, 3–11.

(30) Zhiqiang, A. (2008) Antibody Therapeutics—a mini review. *Trends Bio/Pharmaceutical Ind.* 24–29.

(31) Nimmerjahn, F., and Ravetch, J. V. (2008) Anti-inflammatory actions of intravenous immunoglobulin. *Annu. Rev. Immunol. 26*, 513–33.

(32) Andrew, S. M., and Titus, J. A. (2000) Purification of Immunoglobulin G, in *Current Protocols in Cell Biology*, pp 16.3.1 – 16.3.12.

(33) Daoud-Attieh, M., Chaib, H., Armutcu, C., Uzun, L., Elkak, A., and Denizli, A. (2013) Immunoglobulin G purification from bovine serum with pseudo-specific supermacroporous cryogels. *Sep. Purif. Technol. 118*, 816–822.

(34) Rayner, L. E., Kadkhodayi-kholghi, N., Heenan, R. K., Gor, J., Dalby, P. A., and Perkins, S. J. (2013) The Solution Structure of Rabbit IgG Accounts for Its Interactions with the Fc Receptor and Complement C1q and Its Conformational Stability. *J. Mol. Biol. 425*, 506–523.

(35) Chen, Y., Vaine, M., Wallace, A., Han, D., Wan, S., Seaman, M. S., Montefiori, D., and Wang, S. (2013) A novel rabbit monoclonal antibody platform to dissect the diverse repertoire of antibody epitopes for HIV-1 Env immunogen eesign. *Journals Virol. 87*, 10232–10243.

(36) Hatta, H., Tsuda, K., Akachi, S., Kim, M., and Yamamoto, T. (1993) Productivity and some properties of egg yolk antibody (IgY) against human rotavirus compared with rabbit IgG. *Biosci. Biotechnol. Biochem. 57*, 450–454.

(37) Bagchi, P., and Birnbaum, S. M. (1981) Effect of pH on the adsorption of immunoglobulin G on anionic poly(vinyltoluene) model latex particles. *J Colloid Interface Sci 83*, 460 – 478.

(38) Martínez-Aragón, M., Goetheer, E. L. V., and Haan, A. B. (2009) Host–guest extraction of immunoglobulin G using calix[6]arenas. *Sep. Purif. Technol. 65*, 73–78.

(39) Barroso, T., Temtem, M., Hussain, A., Aguiar-Ricardo, A., and Roque, A. C. A. (2010) Preparation and characterization of a cellulose affinity membrane for human immunoglobulin G (IgG) purification. *J. Memb. Sci. 348*, 224–230.

(40) Radosevich, M., and Burnouf, T. (2010) Intravenous immunoglobulin G: Trends in production methods, quality control and quality assurance. *Vox Sang. 98*, 12–28.

(41) Bresolin, I. T. L., de Souza, M. C. M., and Bueno, S. M. A. (2010) A new process of IgG purification by negative chromatography: adsorption aspects of human serum proteins onto omega-aminodecyl-agarose. *J. Chromatogr. B. Analyt. Technol. Biomed. Life Sci. 878*, 2087–93.

(42) Hober, S., Nord, K., and Linhult, M. (2007) Protein A chromatography for antibody purification. *J. Chromatogr. B 848*, 40–47.

(43) Schrag, D., Corbier, M., and Raimondi, S. (2014) Size exclusion-high-performance liquid chromatography (SEC-HPLC), in *Monoclonal Antibodies: Methods and Protocols, Methods in Molecular Biology* (Ossipow, V., and Fischer, N., Eds.), pp 507–508. Springer Science + Business Media, New York.

(44) Rosa, P. . A. J., Azevedo, A. M., Ferreira, I. . F., Vries, J., Korporaal, R., Verhoef, H. J., Visser, T. J., and Aires-Barros, M. R. (2007) Affinity partitioning of human antibodies in aqueous two-phase systems. *J. Chromatogr. A 1162*, 103–113.

(45) Xu, Y., Souza, M. A. De, Ribeiro-Pontes, M. Z., Vitolo, M., and Pessoa-Jr, A. (2001) Liquid-liquid extraction of pharmaceuticals by aqueous two-phase systems. *Brazilian J. Pharm. Sci. 37*, 305 – 320.

(46) Low, D., O'Leary, R., and Pujar, N. S. (2007) Future of antibody purification. *J. Chromatogr. B 848*, 48–63.

(47) Creagh, A. L., Hasenack, B. B. E., Vanderpadt, A., Sudholter, E. J. R., and Van´t Riet, K. (1994) Vantriet, Separation of amino-acid enantiomers using micellar-enhanced ultrafiltration. *Biotechnol. Bioeng. 44*, 690–698.

(48) Su, C.-K., and Chiang, B. H. (2002) Extraction of Immunoglobulin-G from Colostral Whey by Reverse Micelles. *J. Dairy Sci. 86*, 1639–1645.

(49) Azevedo, A. M., Rosa, P. A. J., Ferreira, I. F., Pisco, A. M. M. O., Vries, J., Korporaal, R., Visser, T. J., and Aires-Barros, M. R. (2009) Affinity-enhanced purification of human antibodies by aqueous two-phase extraction. *Sep. Purif. Technol. 65*, 31–39.

(50) Beijerinck, M. W. (1896). *Zbl. Bakt. II Natur* 698 – 699.

(51) P., A. A. (1958) Particle fractionation in liquid two-phase systems the composition of some phase systems and the behaviour of some model particles in them application to the isolation of cell walls from microorganisms. *Biochim. Biophys. Acta 27*, 378–395.

(52) Raghavarao, K. S. M. S., Ranganathan, T. V., Srinivas, N. D., and Barhate, R. S. (2003) Aqueous two phase extraction-an environmentally benign technique. *Clean Technol. Environ. Policy 5*, 136–141.

(53) Cláudio, A. F. M., Freire, M. G., Freire, C. S. R., Silvestre, A. J. D., and Coutinho, J. a. P. (2010) Extraction of vanillin using ionic-liquid-based aqueous two-phase systems. *Sep. Purif. Technol. 75*, 39–47.

(54) Kammoun, R., Chouayekh, H., Abid, H., Naili, B., and Bejar, S. (2009) Purification of CBS 819.72 α-amylase by aqueous two-phase systems: Modelling using Response Surface Methodology. *Biochem. Eng. J. 46*, 306–312.

(55) Bora, M. M., Borthakur, S., Rao, P. C., and Dutta, N. N. (2005) Aqueous two-phase partitioning of cephalosporin antibiotics: effect of solute chemical nature. *Sep. Purif. Technol. 45*, 153–156.

(56) Porto, T. S., Medeiros e Silva, G. M., Porto, C. S., Cavalcanti, M. T. H., Neto, B. B., Lima-Filho, J. L., Converti, A., Porto, A. L. F., and Jr. Pessoa, A. (2008) Liquid–liquid extraction of proteases from fermented broth by PEG/citrate aqueous two-phase system. *Chem. Eng. Process. 47*, 716–721.

(57) Benavides, J., and Rito-palomares, M. (2008) Practical experiences from the development of aqueous two-phase processes for the recovery of high value biological products. *J. Chem. Technol. Biotechnol. 142*, 133–142.

(58) Hatti-Kaul, R. (Ed.). (2000) Aqueous two-phase systems in Aqueous two-phase systems: methods and protocols.

(59) Rosa, P. . A. J., Ferreira, I. F., Azevedo, A. M., and Aires-Barros, M. R. (2010) Aqueous two-phase systems: A viable platform in the manufacturing of biopharmaceuticals. *J. Chromatogr. A 1217*, 2296–2305.

(60) Quental, M. J. V. (2014) Application of ionic liquids in the concentration of cancer biomarkers. Universidade de Aveiro.

(61) Bernardo. (2013) LYTAG-driven integrative Platform for Purification of Monoclonal Antibodies by Aqueous Two-phase Systems. Técnico Lisboa.

(62) Raja, S., Murty, V. R., Thivaharan, V., Rajasekar, V., and Ramesh, V. (2011) Aqueous two phase systems for the recovery of biomolecules – a review. *Sci. Technol. 1*, 7–16.

(63) Freire, M. G., Cláudio, A. F. M., Araújo, J. M. M., Coutinho, J. A. P., Marrucho, I. M., Canongia, L. J. N., and Rebelo, L. P. N. (2012) Aqueous biphasic systems: a boost brought about by using ionic liquids. *Chem. Soc. Rev. 41*, 4966–4995.

(64) Naganagouda, K., and Mulimani, V. H. (2008) Aqueous two-phase extraction (ATPE): An attractive and economically viable technology for downstream processing of Aspergillus oryzae α-galactosidase. *Process Biochem. 43*, 1293–1299.

(65) Nitsawang, S., Hatti-Kaul, R., and Kanasawud, P. (2006) Purification of papain from Carica papaya latex: aqueous two-phase extraction versus two-step salt precipitation. *Enzyme Microb. Technol. 39*, 1103–1107.

(66) Sulk, B., Birkenmeier, G., and Kopperschläger, G. (1992) Application of phase partitioning and thiophilic adsorption chromatography to the purification of monoclonal antibodies from cell culture fluid. *J. Immunol. Methods 149*, 165–171.

(67) Zijlstra, G. ., Michielsen, M. J., de Gooijer, C. D., van der Pol, L. A., and Tramper, J. (1996) Separation of hybridoma cells from their IgG product using aqueous two-phase systems. *Bioseparation 6*, 201–210.

(68) Andrews, B. A., Nielsen, S., and Asenjo, J. A. (1996) Partitioning and purification of monoclonal antibodies in aqueous two-phase systems. *Bioseparation 6*, 303–306.

(69) Rito-Palomares, M., Dale, C., and Lyddiatt, A. (2000) Generic application of an aqueous two-phase process for protein recovery from animal blood. *Process Biochem. 35*, 665–673.

(70) Azevedo, A. M., Rosa, P. A. J., Ferreira, I. . F., and Aires-Barros, M. R. (2008) Integrated process for the purification of antibodies combining aqueous two-phase extraction, hydrophobic interaction chromatography and size-exclusion chromatography. *J. Chromatogr. A 1213*, 154–161.

(71) Rosa, P. A. J., Azevedo, A. M., Sommerfeld, S., Mutter, M., Aires-Barros, M. R., and Bäcker, W. (2009) Application of aqueous two-phase systems to antibody purification: A multi-stage approach. *J. Biotechnol. 139*, 306–313.

(72) Park, H.-M., Lee, S.-W., Chang, W.-J., and Koo, Y.-M. (2007) Affinity separation by protein conjugated IgG in aqueous two-phase systems using horseradish peroxidase as a ligand carrier. *J. Chromatogr. B 856*, 108–112.

(73) Vargas, M., Segura, A., Herrera, M., Villalta, M., Angulo, Y., Gutiérrez, J. M., León, G., and Burnouf, T. (2012) Purification of IgG and albumin from human plasma by aqueous two phase system fractionation. *Biotechnol. Prog. 28*, 1005–1011.

(74) Wu, Q., Lin, D.-Q., and Yao, S.-J. (2013) Evaluation of poly(ethylene glycol)/hydroxypropyl starch aqueous two-phase system for immunoglobulin G extraction. *J. Chromatogr. B 928*, 106–112.

(75) Rosa, P. A. J., Azevedo, A. M., and Aires-Barros, M. R. (2007) Application of central composite design to the optimisation of aqueous two-phase extraction of human antibodies. *J. Chromatogr. A 1141*, 50–60.

(76) Dhadge, V. L., Rosa, S. A. S. L., Azevedo, A., Aires-Barros, R., and Roque, A. C. A. (2014) Magnetic aqueous two phase fishing: a hybrid process technology for antibody purification. *J. Chromatogr. A 1339*, 59–64.

(77) Liu, Y., Wu, Z., Zhang, Y., and Yuan, H. (2012) Partitioning of biomolecules in aqueous two-phase systems of polyethylene glycol and nonionic surfactant. *Biochem. Eng. J. 69*, 93–99.

(78) Silva, D. F. . C., Azevedo, A. M., Fernandes, P., Chu, V., Conde, J. P., and Aires-Barros, M. R. (2012) Design of a microfluidic platform for monoclonal antibody extraction using an aqueous two-phase system. *J. Chromatogr. A 1249*, 1–7.

(79) Muendges, J., Stark, I., Mohammad, S., Górak, A., and Zeiner, T. (2015) Single stage aqueous two-phase extraction for monoclonal antibody purification from cell supernatant. *Fluid Phase Equilib. 385*, 227–236.

(80) Bernardo, S. C., Azevedo, A. M., and Aires-Barros, M. R. (2014) Integrated plataforms for the clarification and capture of monoclonal antibodies. *Rev. Mex. Ing. Química*.

(81) De Souza, R. L., Campos, V. C., Ventura, S. P. M., Soares, C. M. F., Coutinho, J. A. P., and Lima, Á. S. (2014) Effect of ionic liquids as adjuvants on PEG-based ABS formation and the extraction of two probe dyes. *Fluid Phase Equilib. 375*, 30–36.

(82) Souza, R. L., Ventura, S. P. M., Soares, C. M. F., Coutinho, J. A. P., and Lima, Á. S. (2015) Lipase purification using ionic liquids as adjuvants in aqueous two-phase systems. *Green Chem. 17*, 3026–3034.

(83) Hamzehzadeh, S., and Abbasi, M. (2015) The influence of 1-butyl-3-methyl-imidazolium bromide on the partitioning of L-tyrosine within the {polyethylene glycol 600 + potassium citrate} aqueous biphasic system at T = 298.15 K. *J. Chem. Thermodyn. 80*, 102–111.

(84) Hamzehzadeh, S., and Vasiresh, M. (2014) Ionic liquid 1-butyl-3-methylimidazolium bromide as a promoter for the formation and extraction capability of poly(ethylene glycol)-potassium citrate aqueous biphasic system at T = 298.15 K. *Fluid Phase Equilib. 382*, 80–88.

(85) Marsh, K. N., Boxall, J. A., and Lichtenthaler, R. (2004) Room temperature ionic liquids and their mixtures—a review. *Fluid Phase Equilib. 219*, 93–98.

(86) Earl, M. J., and Seddon, R. K. (2000) Ionic liquids, green solvents for the future. *Pure Appl. Chem. 72*, 1391–1398.

(87) Ranke, J., Stolte, S., Stormann, R., Arning, J., and Jastorff, B. (2007) Design of sustainable chemical products-the example of ionic liquids. *Chem. Rev. 107*, 2183–2206.

(88) Wasserscheid, P., and Welton, T. (2008) Ionic liquids in synthesis.

(89) Welton, T. (1999) Room-temperature ionic liquids. solvents for synthesis and catalysis. *Chem. Rev. 99*, 2071–2084.

(90) Chen, X., Liu, J., and Wang, J. (2010) Ionic liquids in the assay of proteins. *Anal. Methods 2*, 1222 –1226.

(91) Pei, Y., Wang, J., Wu, K., Xuan, X., and Lu, X. (2009) Ionic liquid-based aqueous two-phase extraction of selected proteins. *Sep. Purif. Technol. 64*, 288–295.

(92) Yang, Z., and Pan, W. (2005) Ionic liquids: Green solvents for nonaqueous biocatalysis. *Enzyme Microb. Technol. 37*, 19–28.

(93) Desai, R. K., Streefland, M., Wijffels, R. H., and H. M. Eppink, M. (2014) Extraction and stability of selected proteins in ionic liquid based aqueous two phase systems. *Green Chem. 16*, 2670–2679.

(94) Du, Z., Yu, Y.-L., and Wang, J.-H. (2007) Extraction of proteins from biological fluids by use of an ionic liquid/aqueous two-phase system. *Chemistry (Easton). 13*, 2130–2137.

(95) Quental, M. V, Caban, M., Pereira, M. M., Stepnowski, P., Freire, M. G., Stwosza, W., and Aveiro, U. De. (2015) Research Article 1 Enhanced extraction of proteins using cholinium-based ionic liquids as phase-forming components of aqueous biphasic systems. *Biotechnol. J.* 1–24.

(96) Pereira, M. M., Pedro, S. N., Quental, M. V., Lima, Á. S., Coutinho, J. A. P., and Freire, M. G. (2015) Enhanced extraction of bovine serum albumin with aqueous biphasic systems of phosphonium- and ammonium-based ionic liquids. *J. Biotechnol. 206*, 17–25.

(97) Taha, M., Quental, M. V., Correia, I., Freire, M. G., and Coutinho, J. a. P. (2015) Extraction and stability of bovine serum albumin (BSA) using cholinium-based Good's buffers ionic liquids. *Process Biochem. 50*, 1158–1166.

(98) Cheng, D.-H., Chen, X.-W., Shu, Y., and Wang, J.-H. (2008) Selective extraction/isolation of hemoglobin with ionic liquid 1-butyl-3-trimethylsilylimidazolium hexafluorophosphate (BtmsimPF6). *Talanta 75*, 1270–1278.

(99) Cheng, D.-H., Chen, X.-W., Shu, Y., and Wang, J.-H. (2008) Extraction of cytochrome C by ionic liquid 1-butyl-3-trimethylsilylimidazolium hexafluorophosphate. *Chinese J. Anal. Chem. 36*, 1187–1190.

(100) Desai, R. K., Streefland, M., Wijffels, R. H., and H. M. Eppink, M. (2014) Extraction and stability of selected proteins in ionic liquid based aqueous two phase systems. *Green Chem. 16*, 2670.

(101) Wu, C., Peng, J., Li, J., Bai, Y., Hu, Y., and Lai, G. (2008) Synthesis of poly(ethylene glycol) (PEG) functionalized ionic liquids and the application to hydrosilylation. *Catal. Commun. 10*, 248–250.

(102) Almeida, M. R., Passos, H., Pereira, M. M., Lima, Á. S., Coutinho, J. A. P., and Freire, M. G. (2014) Ionic liquids as additives to enhance the extraction of antioxidants in aqueous two-phase systems. *Sep. Purif. Technol. 128*, 1–10.

(103) Freire, M. G., Neves, C. M. S. S., Lopes, C. N. J., Marrucho, M. I., Coutinho, J. A. . P., and Rebelo, N. P. L. (2012) Impact of self-aggregation on the formation of ionic-liquid-basedaqueous biphasic systems. *J. Chem. Thermodyn. 54*, 7660–7668.

(104) Mourão, T., Cláudio, A. F. M., Boal-Palheiros, I., Freire, M. G., and Coutinho, J. A. P. (2012) Evaluation of the impact of phosphate salts on the formation of ionic-liquid-based aqueous biphasic systems. *J. Chem. Thermodyn. 54*, 398–405.

(105) Merchuk, J. C., Andrews, B. A., and Asenjo, J. A. (1998) Aqueous two-phase systems for protein separation. *J. Chromatogr. B Biomed. Sci. Appl. 711*, 285–293.

(106) Freire, M. G., Pereira, J. F. B., Francisco, M., Rodríguez, H., Rebelo, L. P. N., Rogers, R. D., and Coutinho, J. A. P. (2012) Insight into the interactions that control the phase behaviour of new aqueous biphasic systems composed of polyethylene glycol polymers and ionic liquids. *Chem. - A Eur. J. 18*, 1831–1839.

(107) Lu, Y. M., Yang, Y. Z., Zhao, X. D., and Xia, C. B. (2010) Bovine serum albumin partitioning in polyethylene glycol (PEG)/potassium citrate aqueous two-phase systems. *Food Bioprod. Process. 88*, 40–46.

(108) Glyk, A., Scheper, T., and Beutel, S. (2014) Influence of different phase-forming parameters on the phase diagram of several PEG − salt aqueous two-phase systems. *J. Chem. Eng. Data 59*, 850–859.

(109) Sintra, T. E., Cruz, R., Ventura, S. P. M., and Coutinho, J. A. P. (2014) Phase diagrams of ionic liquids-based aqueous biphasic systems as a platform for extraction processes. *J. Chem. Thermodyn. 77*, 206–213.

(110) Lu, Y.-M., Yang, Y.-Z., Zhao, X.-D., and Xia, C.-B. (2010) Bovine serum albumin partitioning in polyethylene glycol (PEG)/potassium citrate aqueous two-phase systems. *Food Bioprod. Process. 88*, 40–46.

(111) Chemspider, The free chemical database.

(112) Albertsson, P. A. (1986) Partitioning of cell particles and macromolecules. *Wiley–Interscience* 8–38.

(113) Hachem, F., Andrews, B. a., and Asenjo, J. a. (1996) Hydrophobic partitioning of proteins in aqueous two-phase systems. *Enzyme Microb. Technol. 19*, 507–517.

(114) Andrews, B. A., Schmidt, A. S., and Asenjo, J. A. (2005) Correlation for the partition behavior of proteins in aqueous two-phase systems: Effect of surface hydrophobicity and charge. *Biotechnol. Bioeng. 90*, 380–390.

(115) Johansson, G. (1974) Effects of salts on the partition of proteins in aqueous polymeric biphasic systems. *Acta Chem. Scand. B. 28*, 873–882.

(116) Berggren, K., Johansson, H. O., and Tjerneld, F. (1995) Effects of salts and the surface hydrophobicity of proteins on partitioning in aqueous two-phase systems containing thermoseparating ethylene oxide-propylene oxide copolymers. *J. Chromatogr. A 718*, 67–79.

(117) Gonzalez-Tello, P., Camacho, F., and Blazquez, G. (1994) Density and Viscosity of Concentrated Aqueous Solutions of Polyethylene Glycol. *J. Chem. Eng. Data 39*, 611–614.

(118) Modlin, R. F., Alredb, P. A., and Tjemeldb, F. (1994) Utilization of temperature-induced phase separation for the purification of ecdysone and 20-hydroxyecdysone from spinach *668*, 229–236.

(119) Carlsson, M., Linse, P., and Tjerneld, F. (1993) Temperature-dependent protein partitioning in two-phase aqueous polymer systems. *Macromolecules 26*, 1546–1554.

(120) Asenjo, J. A., Schmidt, A. S., Hachem, F., and Andrews, B. A. (1994) Model for predicting the partition behaviour of proteins in aqueous two-phase systems. *J. Chromatogr. A* 47–54.

(121) Cláudio, A. F. M., Ferreira, A. M., Shahriari, S., Freire, M. G., and Coutinho, J. A. P. (2011) Critical assessment of the formation of ionic-liquid-based aqueous two-phase systems in acidic media. *J. Phys. Chem. B 115*, 11145–11153.

(122) Zhang, Y., and Cremer, P. S. (2006) Interactions between macromolecules and ions: the Hofmeister series. *Curr. Opin. Chem. Biol. 10*, 658–663.

(123) Yang, Z. (2009) Hofmeister effects: an explanation for the impact of ionic liquids on biocatalysis. *J. Biotechnol. 144*, 12–22.

(124) Patel, R., Kumari, M., and Khan, A. B. (2014) Recent advances in the applications of ionic liquids in protein stability and activity: a review. *Appl. Biochem. Biotechnol. 172*, 3701–3720.

(125) Grudniewska, A., Gniłka, R., and Wawrzeńczyk, C. (2010) Enantioselectivity of hydroxylation of racemic piperitone by fungi. *Chirality 22*, 929–935.

(126) Ventura, S. P. M., Santos, L. D. F., Saraiva, J. A., and Coutinho, J. A. P. (2012) Ionic liquids microemulsions: the key to Candida antarctica lipase B superactivity. *Green Chem. 14*, 1547–1806.

Appendix A

Calibration curve

Figure A.1 depicts the calibration curve (absorbance *vs.* concentration of total amount of protein). The calibration curve was made with rabbit IgG.

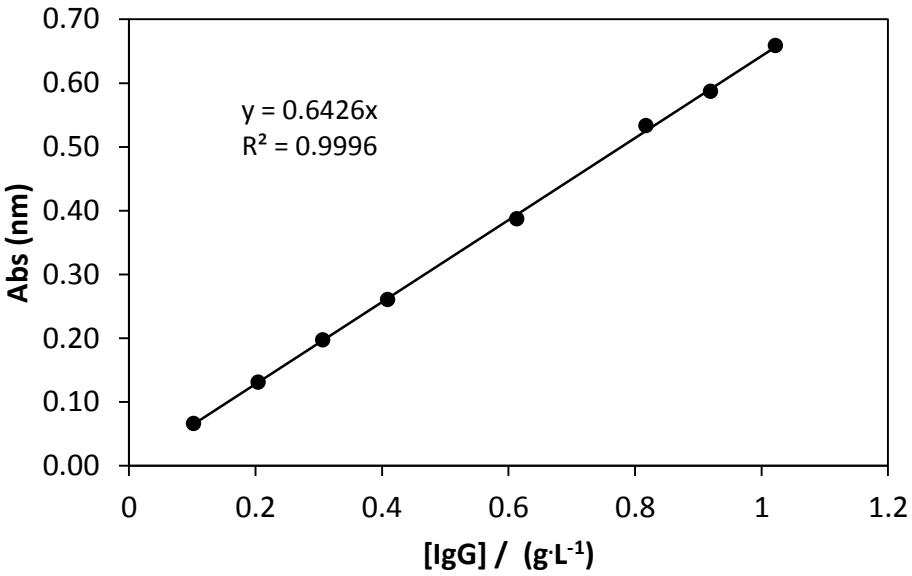

Figure A. 1: Calibration curve for total amount of protein at λ = 280 nm.

Appendix B
Experimental binodal data

The experimental weight fraction data for the phase diagrams of the systems composed of PEG + $C_6H_5K_3O_7$/$C_6H_8O_7$ + H_2O at pH≈7 are presented in Table B. 1 to Table B. 4.

Table B. 1: Experimental weight fraction data for the system composed of PEG (1) + $C_6H_5K_3O_7$/$C_6H_8O_7$ (2) + H_2O (3) at 25 ^oC and at atmospheric pressure.

PEG 400					
100 w_1	**100 w_2**	**100 w_1**	**100 w_2**	**100 w_1**	**100 w_2**
17.6667	0.1208	1.0534	1.0162	0.5310	1.4661
10.2530	0.1774	1.0237	1.0374	0.5184	1.4845
5.9874	0.2684	0.9930	1.0568	0.5110	1.4868
3.7506	0.3644	0.9370	1.1047	0.4969	1.5076
2.9612	0.4313	0.9028	1.1277	0.4854	1.5174
2.7227	0.4547	0.8759	1.1521	0.4719	1.5424
2.4975	0.4891	0.8329	1.1895	0.4527	1.5662
2.2364	0.5405	0.8172	1.1940	0.4132	1.6276
2.1893	0.5457	0.7986	1.2099	0.3927	1.6530
2.1194	0.5648	0.7877	1.2150	0.3657	1.6916
2.0110	0.5975	0.7761	1.2240	0.3497	1.7120
1.8958	0.6356	0.7696	1.2299	0.3416	1.7185
1.8250	0.6473	0.7485	1.2454	0.3078	1.7760
1.7728	0.6671	0.7324	1.2605	0.2841	1.8076
1.7073	0.6871	0.7221	1.2670	0.1526	2.8601
1.5861	0.7519	0.7021	1.2858	0.1897	1.9307
1.4683	0.7879	0.6973	1.2877	0.3059	1.6282
1.3953	0.8211	0.6906	1.2950	0.7904	1.0007
1.3523	0.8397	0.6636	1.3195		
1.3358	0.8470	0.6554	1.3273		
1.2931	0.8659	0.6446	1.3380		
1.2756	0.8792	0.6368	1.3435		
1.2198	0.9177	0.6206	1.3675		
1.2061	0.9251	0.6122	1.3721		
1.1685	0.9480	0.5886	1.3928		

Table B. 2: Experimental weight fraction data for the system composed of PEG (1) + $C_6H_5K_3O_7$/$C_6H_8O_7$ (2) + H_2O (3) at 25 °C and at atmospheric pressure.

PEG 600							
100 w_1	**100 w_2**	**100 w_1**	**100 w_2**	**100 w_1**	**100 w_2**	**100 w_1**	**100 w_2**
7.0842	0.0504	0.5065	0.7261	0.2511	1.0857	0.1570	1.2830
3.6416	0.1005	0.4980	0.7351	0.2462	1.0968	0.1517	1.2921
3.2769	0.1191	0.4896	0.7398	0.2438	1.1005	0.1456	1.3244
1.6936	0.2361	0.4769	0.7605	0.2409	1.1047	0.1393	1.3347
1.5467	0.2667	0.4640	0.7795	0.2391	1.1092	0.1364	1.3442
1.4595	0.2727	0.4526	0.7877	0.2356	1.1148	0.1303	1.3504
1.3641	0.2941	0.4394	0.8035	0.2323	1.1214	0.1250	1.3820
1.2798	0.3052	0.4272	0.8201	0.2288	1.1278	0.1218	1.3859
1.2184	0.3214	0.4165	0.8278	0.2249	1.1379	0.1188	1.3951
1.1758	0.3383	0.4076	0.8436	0.2215	1.1431	0.1099	1.4279
1.1393	0.3468	0.4023	0.8455	0.2171	1.1563	0.0963	1.4767
1.0986	0.3628	0.3983	0.8518	0.2124	1.1644	0.1450	1.8285
1.0668	0.3778	0.3936	0.8569	0.2087	1.1707	0.2073	1.6047
1.0319	0.3921	0.3894	0.8612	0.2061	1.1777	0.2786	1.4788
0.9945	0.3997	0.3836	0.8700	0.2034	1.1850	0.3238	1.3873
0.9615	0.4122	0.3728	0.8831	0.2012	1.1862	0.3769	1.3320
0.9423	0.4193	0.3656	0.8930	0.1982	1.1926	0.3988	1.2840
0.9232	0.4266	0.3595	0.902	0.1952	1.1980	0.4856	1.2068
0.8989	0.4389	0.3550	0.9078	0.1915	1.2088	0.5353	1.1413
0.8625	0.4542	0.3515	0.9128	0.1884	1.2111	0.5673	1.1112
0.8301	0.4768	0.3465	0.9226	0.1842	1.2228		
0.8010	0.4855	0.3426	0.9252	0.1810	1.2280		
0.7804	0.5001	0.3386	0.9311	0.1773	1.2384		
0.7644	0.5113	0.3344	0.9374	0.1720	1.2518		
0.7546	0.5151	0.3313	0.9411	0.1696	1.2538		
0.7309	0.5270	0.3274	0.9476	0.1654	1.2683		

Table B. 3: Experimental weight fraction data for the system composed of PEG (1) + $C_6H_5K_3O_7/C_6H_8O_7$ (2) + H_2O (3) at 25 °C and at atmospheric pressure.

PEG 1000		**PEG 2000**		**PEG 4000**	
100 w_1	**100 w_2**	**100 w_1**	**100 w_2**	**101 w_1**	**101 w_2**
0.9761	0.3060	0.2650	0.2429	0.1034	0.2536
0.8536	0.3474	0.2562	0.2528	0.0902	0.2830
0.7166	0.3576	0.2470	0.2631	0.0798	0.3113
0.6533	0.3794	0.2388	0.2711	0.0694	0.3386
0.6049	0.3948	0.2316	0.2818	0.0503	0.3996
0.5622	0.4253	0.2218	0.2898	0.0436	0.4386
0.530	0.4358	0.1624	0.3737	0.0390	0.4690
0.0542	1.2678	0.1593	0.3782	0.0375	0.4752
0.0666	1.1863	0.1548	0.3821	0.0350	0.4969
0.0798	1.1314	0.1182	0.4583	0.0340	0.5059
0.0885	1.1064	0.1162	0.4625	0.0331	0.5082
0.1016	1.0688	0.1145	0.4681	0.0197	0.6183
0.1103	1.0384	0.1106	0.4821	0.0225	0.5952
0.1175	1.0149	0.1052	0.4976	0.0244	0.5789
0.1287	0.9863	0.0259	0.8948	0.0264	0.5623
0.1352	0.9708	0.0259	0.8948	0.0324	0.5245
0.1401	0.9574	0.0366	0.7975	0.0344	0.5059
0.1431	0.9479	0.0401	0.7755	0.0364	0.4904
		0.0712	0.6352		
		0.0932	0.5546		

Table B. 4: Experimental weight fraction data for the system composed of PEG (1) + $C_6H_5K_3O_7/C_6H_8O_7$ (2) + H_2O (3) at 25 °C and at atmospheric pressure.

PEG 6000						PEG 8000			
100 w_1	100 w_2	100 w_1	100 w_2	100 w_1	100 w_2	100 w_1	100 w_2	100 w_1	100 w_2
0.0691	0.2680	0.0113	0.5950	0.0070	0.6646	0.0054	0.6103	0.0065	0.5743
0.0348	0.3721	0.0111	0.6051	0.0067	0.6667	0.0065	0.5848	0.0072	0.5657
0.0297	0.3984	0.0108	0.6100	0.0066	0.6628	0.0083	0.5526	0.0078	0.5550
0.0250	0.4360	0.0105	0.6131	0.0064	0.6721	0.0098	0.5293	0.0084	0.5424
0.0245	0.4402	0.0103	0.6081	0.0063	0.6731	0.0123	0.4911		
0.0197	0.4931	0.0102	0.6210	0.0062	0.6765	0.0148	0.4558		
0.0186	0.4972	0.0100	0.6155	0.0060	0.6789	0.0169	0.4287		
0.0182	0.5072	0.0098	0.6219			0.0057	2.8291		
0.0178	0.5113	0.0096	0.6272			0.0029	0.6626		
0.0173	0.5137	0.0094	0.6216			0.0036	0.6423		
0.0170	0.5165	0.0093	0.6243			0.0044	0.6247		
0.0167	0.5228	0.0091	0.6281			0.0051	0.6056		
0.0163	0.5233	0.0090	0.6270			0.0058	0.5891		
0.0161	0.5288	0.0089	0.6337			0.0065	0.5743		
0.0158	0.5330	0.0087	0.6394			0.0072	0.5657		
0.0154	0.5460	0.0086	0.6329			0.0078	0.5550		
0.0149	0.5505	0.0085	0.6407			0.0084	0.5424		
0.0146	0.5443	0.0083	0.6478			0.0232	0.3923		
0.0143	0.5583	0.0080	0.6423			0.0225	0.3970		
0.0139	0.5560	0.0079	0.6472			0.0057	2.8291		
0.0135	0.5694	0.0078	0.6513			0.0029	0.6626		
0.0130	0.5783	0.0076	0.6474			0.0036	0.6423		

The experimental weight fraction data for the phase diagrams of the systems composed of PEG 400 + $C_6H_5K_3O_7$/$C_6H_8O_7$ at different pH values + H_2O are presented in Table B. 5 to Table B. 6.

Table B. 5: Experimental weight fraction data for the systems composed of PEG 400 (1) + $C_6H_5K_3O_7$/$C_6H_8O_7$ (2) + H_2O (3) at different pH values, at 25 °C and atmospheric pressure.

pH≈5		pH≈6			
100 w_1	100 w_2	100 w_1	100 w_2	100 w_1	100 w_2
97.6785	1.1474	83.1460	3.1973	26.1275	24.0347
59.4245	10.5023	80.2857	3.9381	27.1130	23.3590
54.8208	12.4952	74.0831	5.5981	27.8631	22.8964
51.8751	13.4461	70.2003	6.3838	28.4717	22.4577
43.1889	17.5656	67.5146	7.2412	29.0311	21.9991
37.4680	20.1883	62.7472	8.2251	30.0644	21.4199
29.6068	25.8032	60.1183	8.7867	30.7338	20.9344
79.5788	4.5648	52.5302	11.5347	31.3464	20.2928
75.1961	5.3173	42.9395	14.2884	32.5943	19.6152
42.5024	17.6484	41.0086	15.0556	33.0527	19.2490
37.5837	20.4752	39.3498	15.8188	33.9441	18.5133
43.8210	17.3961	37.4010	16.9016	34.8239	18.0871
38.0120	20.3881	8.3076	39.0424	35.6767	17.4873
35.6522	21.0005	10.2215	36.9386		
31.98544	24.1809	11.0343	36.0117		
32.41776	23.6163	11.8581	35.3441		
33.04591	23.1484	12.6053	34.5915		
34.39002	22.2523	13.2279	33.8544		
35.73221	21.4667	15.3038	32.1482		
39.17455	19.1808	16.7716	31.1742		
24.76493	30.11694	17.2677	30.5668		
21.7746	32.0034	18.5333	29.6867		
20.3919	34.5012	19.1007	29.1624		
25.2329	28.9867	20.3021	28.3650		
16.3097	37.7884	21.5244	27.5649		
18.7841	35.7096	21.9908	27.1238		
17.5897	36.5537	22.9232	26.4286		
12.0404	41.5647	23.9513	25.7182		
		24.2902	25.2971		
		25.1437	24.6179		

Table B. 6: Experimental weight fraction data for the systems composed of PEG 400 (1) + $C_6H_5K_3O_7$/$C_6H_8O_7$ (2) + H_2O (3) at different pH values, at 25 °C and atmospheric pressure.

pH≈9				pH≈8			
100 w_1	100 w_2	100 w_1	100 w_2	100 w_1	100 w_2	100 w_1	100 w_2
98.7614	0.6114	19.6993	25.3901	97.9816	1.0131	6.0589	36.1366
68.2447	3.1421	18.8710	26.0018	72.0986	2.9437	7.0630	35.2505
65.9899	3.8872	18.3604	26.2245	65.5590	4.2215	9.0933	33.1761
63.3480	4.3566	17.8041	26.6026	61.8489	5.2348	9.9558	32.3053
61.1248	5.2798	17.4656	26.8562	58.1287	6.1471	10.9065	31.6091
57.1765	6.8965	16.6855	27.3949	53.9687	7.3423	11.7741	30.9423
54.4698	7.5474	16.3474	27.6280	51.7503	8.0110	12.5534	30.3797
53.3535	7.8675	16.1222	27.7605	46.5439	10.5737	13.3199	29.8972
50.7736	8.8696	15.7539	28.0582	44.9058	11.0891	13.9490	29.2169
49.7684	9.1850	15.5798	28.1564	43.1049	12.0416	15.2438	28.3406
46.7201	10.6741	15.2734	28.3902	41.6065	12.7035	15.8502	27.7407
44.9089	11.6286	15.0137	28.5631	40.3051	13.2035	17.2340	26.9222
43.2403	12.1418	14.8760	28.5919	38.3276	14.2975	17.8247	26.4605
42.1962	12.5506	14.5414	28.8819	36.8786	14.7359	18.8281	25.7318
40.4663	13.1536	2.4456	48.1525	33.2908	16.7460		
39.4923	13.5933	3.7524	44.0195	32.3498	17.2076		
38.1205	14.3601	4.6473	40.0228	31.8512	17.4923		
37.4959	14.5110	5.5669	38.1322	31.2476	17.8160		
35.8609	15.6126	6.6937	36.3331	30.1857	18.6230		
34.5416	16.0606	7.4991	34.8308	29.5314	18.9394		
33.8126	16.3824	8.9759	33.0886	28.9074	19.1716		
32.9396	16.9120	10.7990	31.8381	28.0889	19.6419		
32.0742	17.4605	11.5234	31.1063	27.5907	19.9676		
30.7456	18.0696	12.3085	30.3982	26.8083	20.5204		
29.1959	19.0198	13.9001	29.3979	26.3774	20.8019		
27.6533	20.0223	14.9116	28.6416	25.9860	21.0619		
26.5636	20.6568	16.4486	27.7227	25.2994	21.4896		
24.8188	21.8903	17.0294	27.1178	24.8228	21.8130		
24.2601	22.2001	19.6993	25.3901	24.4753	22.0550		
23.7156	22.5333	18.8710	26.0018	23.9810	22.3626		
22.8205	23.2478	18.3604	26.2245	23.5928	22.6428		
22.4224	23.4550	17.8041	26.6026	23.2114	22.9108		
21.8741	23.8240	17.4656	26.8562	22.8346	23.1516		
98.7614	0.6114	16.6855	27.3949	22.3768	23.4472		
68.2447	3.1421			21.8416	23.7413		
65.9899	3.8872			21.4612	24.0039		
63.3480	4.3566			21.0831	24.2745		
61.1248	5.2798			20.7018	24.5273		
57.1765	6.8965			20.2810	24.8188		

Appendix C

Additional experimental data

Additional data for the ABS composed of PEG + $C_6H_5K_3O_7/C_6H_8O_7$ + H_2O at pH ≈ 7 are shown in Figure C.1 and Table C. 1.

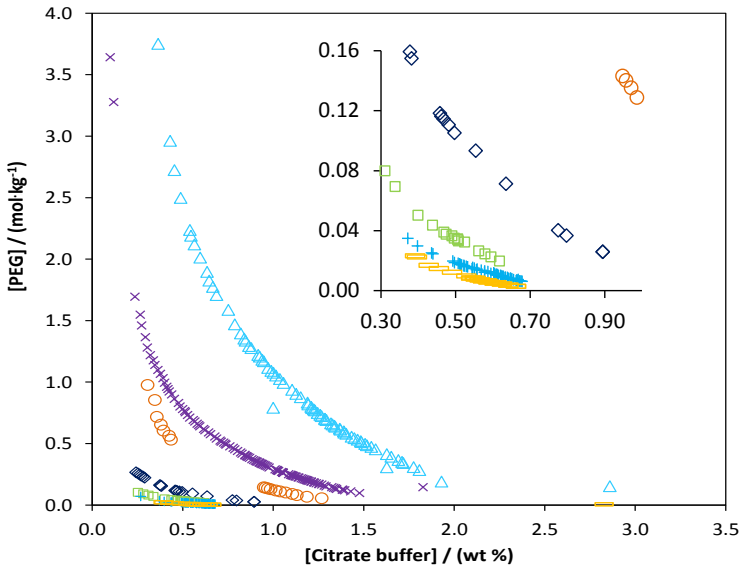

Figure C. 1: Evaluation of the molecular weight of PEG in ABS composed of PEG + $C_6H_5K_3O_7/C_6H_8O_7$ + H_2O: PEG 400 (△); PEG 600 (×); PEG 1000 (○); PEG 2000 (◇); PEG 4000 (□); PEG 6000 (+) PEG 8000 (▫).

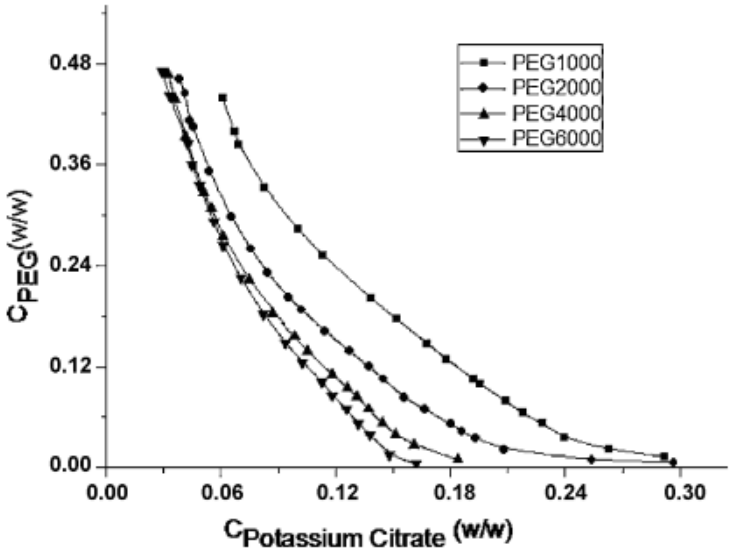

Figure C. 2: Phase diagrams for PEG–potassium citrate systems with different PEG molecular weights at 30 °C *(107)*.

Table C. 1: Critical points of the investigated systems PEG (400, 600, 1000, 2000, 4000, 6000 and 8000) + $C_6H_5K_3O_7/C_6H_8O_7$ at pH ≈ 7 + H_2O.

Critical Points (wt %)		
MW PEG	**$C_6H_5K_3O_7/C_6H_8O_7$**	**PEG**
400	23.86	22.98
600	22.96	15.29
1000	18.09	19.22
2000	15.53	12.74
4000	12.23	13.94
6000	12.00	12.42
8000	12.48	9.85

Additional data for the ABS composed of PEG 400 + $C_6H_5K_3O_7/C_6H_8O_7$ + H_2O at different pH values are shown in Figure C.3 and Table C.2.

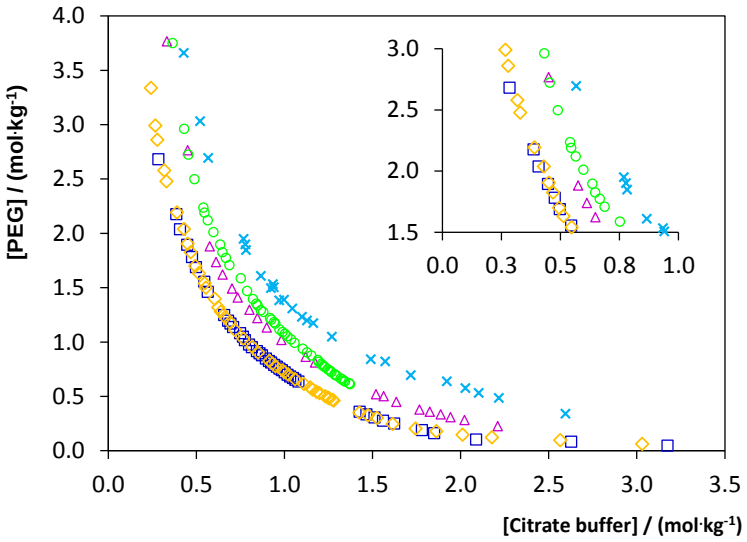

Figure C. 3: Evaluation of the molecular weight of PEG in ABS composed of PEG 400 + $C_6H_5K_3O_7/C_6H_8O_7$ + water at 25 °C and atmospheric pressure at different pH: pH 5(×), pH 6 (△), pH 7 (○), pH 8 (□)and pH 9 (◇).

Table C. 2: Critical points of the investigated systems (PEG 400+ $C_6H_5K_3O_7/C_6H_8O_7$ + H_2O) at different pH values.

Critical Points / (wt %)		
pH	**PEG 400**	**$C_6H_5K_3O_7/C_6H_8O_7$**
5	13.87	39.29
6	20.98	27.51
7	22.24	24.35
8	24.23	22.11
9	26.40	20.80

Appendix D

Extraction efficiencies of IgG: experimental data

Experimental data for extraction efficiency (EE_{IgG} %) and partition coefficient of IgG (K) and extraction yield in the top phase (Y_{IgG} %), for systems composed of PEG + $C_6H_5K_3O_7$/$C_6H_8O_7$ at pH ≈7 + H_2O at different times of extraction and rest from Table D.1 to Table D.2.

Table D. 1: Results of partition coefficient, extraction efficiency and extraction yield of rabbit IgG, with the associated standard deviation, using systems formed by PEG 400 and 8000. Times of equilibrium ranging from 10 to 120 min, before 10 min of centrifugation at 1000 rpm, and 300 and 720 min of equilibrium time without centrifugation.

PEG	Time (min)	K_{IgG}	Standard deviation	EE_{IgG} %	Standard deviation	Y_{IgG} %	Standard deviation
400	**10**	11.44	0.83	91.93	0.56	41.54	4.44
	30	7.20	0.15	87.80	0.22	40.32	2.17
	60	17.26	5.92	93.88	1.98	39.41	3.91
	120	22.72	4.34	95.61	0.93	40.32	2.87
	300	7.55	1.95	87.66	2.82	42.18	0.80
	720	12.06	1.79	92.21	0.98	46.21	2.71
8000	**10**	1.45	0.15	59.11	2.43	34.08	2.62
	30	0.32	0.13	23.23	7.65	12.24	6.88
	60	1.03	0.08	50.74	1.97	23.71	2.06
	120	0.41	0.15	38.17	7.43	7.15	5.47
	300	1.31	0.08	56.61	1.58	41.79	4.94
	720	2.10	0.69	66.11	7.54	39.95	4.35

Table D. 2: : Results of partition coefficient, extraction efficiency and extraction yield of rabbit IgG, with the associated standard deviation, using systems formed by PEG 400, 2000 and 8000. Times of equilibrium ranging from 10 to 120 min, before 10 min of centrifugation at 1000 rpm, and 300 and 720 min of equilibrium time.

PEG	Time (min)	K_{IgG}	Standard deviation	EE_{IgG} %	Standard deviation	Y_{IgG} %	Standard deviation
400	**60**	17.26	5.92	93.88	1.98	37.54	3.91
	120	22.72	4.34	95.61	0.93	40.32	2.87
	180	18.86	7.75	94.17	2.13	72.23	3.25
2000	**60**	3.01	1.20	72.58	8.24	43.58	6.88
	120	2.58	0.50	71.58	3.66	59.59	4.09
	180	2.04	0.31	66.77	3.43	21.17	0.61
8000	**60**	1.03	0.08	50.74	1.97	23.71	2.06
	120	0.41	0.15	38.17	7.43	7.15	5.47
	180	0.73	0.06	42.17	1.89	21.80	0.53

Experimental data for the extraction efficiency (EE_{IgG} %), partition coefficient (K) and extraction yield (Y_{IgG} %) of rabbit IgG using the systems composed of $C_6H_5K_3O_7/C_6H_8O_7$ + H_2O + PEGs of different molecular weights at pH ≈7 are presented in Table D.3.

Table D. 3: : Results of partition coefficient, extraction efficiency and extraction yield of rabbit IgG, with the associated standard deviation, using systems formed by PEG 400, 600, 1000, 2000, 4000, 6000 and 8000. Times of equilibrium ranging from 10 to 120 min, before 10 min of centrifugation at 1000 rpm.

PEG	Time (min)	K_{IgG}	Standard deviation	EE_{IgG} %	Standard deviation	Y_{IgG} %	Standard deviation
400	**120 1000 rpm**	22.72	4.34	95.61	0.93	40.32	2.87
600		14.10	1.19	97.79	3.12	44.41	0.74
1000		8.69	1.27	89.50	1.37	43.82	7.69
2000		3.01	1.20	54.49	9.86	43.58	6.88
4000		1.93	0.46	64.95	5.95	32.96	7.05
6000		1.99	0.26	82.55	9.07	41.00	3.52
8000		0.41	0.15	38.17	7.43	7.05	5.47

The experimental data for extraction efficiency (EE_{IgG} %), partition coefficient (K), and yield (Y_{IgG} %) of rabbit IgG in the systems composed of PEG 400 + $C_6H_5K_3O_7/C_6H_8O_7$ + H_2O at different pH values are shown in Table D.4.

Table D. 4: Extraction efficiency (EEI_{gG} %), partition coefficient (K), and yield (Y_{IgG} %) of rabbit IgG in the systems composed of PEG 400 + $C_6H_5K_3O_7/C_6H_8O_7$ + H_2O at different pH values.

PEG	pH	K_{IgG}	Standard deviation	EE_{IgG} %	Standard deviation	Y_{IgG} %	Standard deviation
400	**6**	30.22	2.05	96.68	3.35	45.65	3.33
	7	22.72	4.34	95.61	0.93	40.32	2.87
	8	36.04	1.42	97.30	1.69	49.40	1.69
	9	41.64	5.54	97.07	2.56	43.26	2.28

The experimental data for extraction efficiency (EE_{IgG}%), partition coefficient (K) and extraction yield (Y_{IgG} %) of rabbit IgG in the systems composed of PEG 400 + $C_6H_5K_3O_7/C_6H_8O_7$ at pH ≈7 + H_2O and 5% of different ILs as adjuvants are shown in Table D.5 and Table D.6.

Table D. 5: Extraction efficiency (EE_{IgG} %), partition coefficient (K), and yield (Y_{IgG} %) of rabbit IgG in the systems composed of PEG 400 + $C_6H_5K_3O_7/C_6H_8O_7$ + H_2O + 5% of [C_4mim]-based ILs (IL anions: Cl^-, $[Tos]^-$, Br^-, $[CH_3CO_2]^-$, $[N(CN)_2]^-$) at pH ≈ 7.

ILs	K_{IgG}	Standard deviation	EE_{IgG} %	Standard deviation	Y_{IgG} %	Standard deviation
No IL	22.72	4.34	95.61	0.93	40.32	2.87
[C_4mim]Cl	60.00	---	100.00	---	36.89	9.31
[C_4mim][TOS]	60.00	---	100.00	---	36.83	6.73
[C_4mim]Br	60.00	---	89.73	10.27	55.06	10.01
[C_4mim]Ac	60.00	---	100.00	---	26.81	5.90
[C_4mim][$N(CN)_2$]	60.00	---	93.13	8.00	31.13	1.41

Table D. 6: Extraction efficiency (EE_{IgG} %), partition coefficient (K), and yield (Y_{IgG} %) of rabbit IgG in the systems composed of PEG 400 + $C_6H_5K_3O_7/C_6H_8O_7$ + H_2O + 5% of 5% of [$C_n$mim]Cl ILs (with n= 2, 4, 6, 8, 10, 12, 14) at pH ≈ 7.

[$C_n$mim]Cl	K_{IgG}	Standard deviation	EE_{IgG} %	Standard deviation	Y_{IgG} %	Standard deviation
No IL	22.72	4.34	95.61	0.93	40.32	2.87
[C_2mim]Cl	60.00	---	100.00	---	25.44	9.85
[C_4mim]Cl	60.00	---	100.00	---	36.89	9.31
[C_6mim]Cl	60.00	---	100.00	---	30.37	3.42
[C_8mim]Cl	4.79	---	82.70	0.82	72.35	5.87
[C_{10}mim]Cl	52.96	---	94.61	3.70	81.24	11.79
[C_{12}mim]Cl	60.00	---	100.00	---	30.01	5.50
[C_{14}mim]Cl	60.00	---	97.63	3.36	41.23	5.17